Abstract

The fatigue crack growth and low cycle fatigue behavior of two P/M superalloys, René 95 and Astroloy, in the HIP condition, has been determined. Test variables included frequency, temperature, environment, and hold times at peak tensile loads (or strains). Crack initiation sites were identified in both alloys. Crack growth rates were shown to increase in argon with decreasing frequency or with the imposition of hold times. This behavior was attributed to the effect of oxygen in the argon. Auger analyses was performed on oxide films formed in argon. Low cycle fatigue lives also were degraded by tensile hold, contrary to previous reports in the literature. The role of environment in low cycle fatigue behavior was discussed.

CREEP-FATIGUE INTERACTIONS IN NICKEL-BASE SUPERALLOYS

I. INTRODUCTION

New turbine disk materials with higher strength and higher temperature capabilities permit achievement of improved efficiency and superior performance from aircraft engines. Hot isostatically pressed (HIP) alloys prepared from powder offer good potential for cost reduction as forging operations can be eliminated and material losses are reduced. However, powdered materials often suffer from premature failure associated with non-metallic inclusions. Further, the extent to which fatigue lives and crack growth rates of P/M superalloys may be affected by creep-fatigue-environment interactions has not been well established. This investigation deals with assessment of the cyclic crack growth behavior of two P/M Ni-base superalloys, primarily in an argon atmosphere. Two representative turbine disk materials were chosen for study. René 95 and Astroloy. In the aircraft gas turbine, disk alloys have to sustain high stresses at temperatures around 650°C. Life may be limited by fatigue crack growth (FCG) from an existing flaw, or by low cycle fatigue (LCF) behavior. Therefore, both FCG and LCF experiments were carried out at several temperatures in the same range, 575-725°C.

II. PURPOSE AND SCOPE

The aim of this study was to determine the influence of environment, frequency, hold times and temperature on FCG and LCF behavior of two P/M Ni-base superalloys. The prevailing materials degradation mechanisms were to be explored and appropriate life prediction methods were to be developed.

III. EXPERIMENTAL PROCEDURE

Table I describes the composition, mechanical properties and microstructures

of the alloys selected for this program, while Figs. 1 and 2 show the microstructures of Astroloy and René 95, respectively. All material was received from NASA-Lewis. Prior to heat treatment, 25mm (1") thick disks were cut from as-HIP cylinders. Compact tension and cylindrical low cycle fatigue specimens were machined from the centers and peripheries of the disks, respectively.

Fatigue crack growth tests were conducted on a closed loop servohydraulic MTS machine with load capacity of 10 tons, temperature capability up to 1000°C and vacuum capacity with a diffusion pump up to 5×10^{-5} torr. These tests were performed at 575°C, 650°C and 725°C respectively with R ratio (K_{min}/K_{max}) equal to 0.05. All tests were performed under ramp waveform, load-controlled conditions. A dc-potential drop technique was used to monitor crack length at the high temperatures. In this technique, a constant current is passed through the specimen (5-7 Amps) and the voltage is measured from probes attached on either side of the crack. As the crack grows, higher resistance due to the increased current path causes an increase in potential drop. Actual crack lengths are obtained from potential drop data by using a standard conversion formula.[1] The validity of such a conversion was tested by running a calibration test in which cycling was stopped at an intermediate crack length and the equivalent crack length was measured at room temperature. Each specimen was precracked at room temperature using 20Hz frequency and load levels ΔP=600-700 lbs. Initial crack lengths were accurately measured under a microscope at 400X. After each test a plot of crack growth rate, da/dN, vs. stress intensity range, ΔK, was obtained. The fracture surface of each specimen was then examined by SEM.

Table II shows the test matrix for FCG experiments. The tests were run

under four different sets of conditions:

1. In argon: to determine temperature and frequency effects.
2. In air: to determine environmental effects by comparison with argon data.
3. In argon, with hold times: to evaluate the extent of any creep-fatigue interaction. These data were compared with those under continuous cycling conditions to differentiate between pure fatigue and creep-fatigue in argon. As will be seen below, environmental attack occurred in argon.
4. In air, with hold times: to produce creep-fatigue-environment interactions under oxidizing conditions.

Low cycle fatigue tests were conducted at 650°C and 725°C in argon with HIP Astroloy and HIP René 95. The cylindrical specimens (gage length 0.76cm, gage diameter 0.3cm), see Fig. 3, were machined by turning and grinding. (For René 95 a tapered shoulder was used; other specimen dimensions were the same). Tool marks were removed by smoothing with emery cloth using up to 0.3μm pure Al_2O_3 powder. Split-type threaded grips were used to hold the specimen and care was taken to eliminate the distortion of specimens during mounting.

All LCF tests were performed under total axial strain-controlled conditions in argon on an MTS closed-loop high temperature system. The cyclic tests were performed at a frequency of 0.33Hz (20 cpm). In some cases, a hold time of 2 min. was imposed at maximum tensile strain. Total strain range was varied from 1.5-2.7%; R=-1 (fully reversed). Since plastic strain range per cycle changed continuously during the test, the plastic strain range at $N_{f/2}$ was used for data plotting and for comparison with other data.

Fracture surfaces were examined by SEM to identify crack initiation sites and to determine crack propagation mechanisms.

EXPERIMENTAL RESULTS

A - Fatigue Crack Growth

Figs. 4-7 show typical FCG results obtained for Astroloy. It is difficult to distinguish between stages I, II and III in any of these curves. There is no significant change in growth rate with temperature between 575 and 725°C, Fig. 4. Both at 575°C and 650°C there is a notable frequency effect, see Fig. 5, with lower frequency causing more rapid crack growth. FCG rates were higher for the specimens tested in air than in argon, Fig. 6. Specimens tested in both environments showed substantial oxidation. The hold time of just two minutes (120 s), Fig. 7, increased the FCG rate by almost two orders of magnitude.

Specimens tested at room temperature showed brittle striations, Fig. 8a), whereas ductile striations were noted for high temperature tests, Fig. 8b). All fractures were transgranular except in the sample tested with a hold time. The latter displayed mixed TG-IG cracking, secondary cracking and a significant amount of oxidation only at the fresh surface (not in the precracked region).

FCG results have been obtained for René 95 at 650°C as a function of frequency and environment. Fig. 9 shows significantly more rapid crack growth in argon than in vacuum of 10^{-4} to 10^{-5} torr. A strong frequency effect in argon is noted also, see Fig. 10. A two min. hold in argon caused a dramatic shift upward in crack growth rate, see Fig. 11, as was the case for Astroloy, Fig. 7. An experiment with six min. hold times produced no further increase in crack growth rate.

A small deleterious effect of decreasing frequency was noted in the air tests. The results at 0.1Hz in vacuum were about equivalent to those at 1Hz in argon. In all continuously cycled test specimens the fracture path was

transgranular.

In general, crack growth rates were slightly higher in the case of René 95 than in Astroloy for identical test conditions; total life of René 95 under equivalent FCG conditions is about 1/2 - 2/3 of that of Astroloy. In both alloys occasional voids (5-10μm) have been noted, perhaps due to the original porosity of the P/M alloys.

Crack growth in René 95 at 650°C in argon was transgranular with brittle striations, see Fig. 12. The two min. hold time produced intergranular fractu as may be seen clearly in Fig. 13; the precrack region (produced at 25°C) is TG, while the crack morphology produced during the hold time cycling at 650°C is IG.

A changing waveform test was carried out on René 95 according to the scheme shown in Fig. 14. The crack growth rates resulting from the waveform variations are shown in Fig. 15. Tensile holds were interspersed between cycles of constant frequency (1 or 20Hz). The resulting fracture surfaces were always transgranular during continuous cycling, but changed to intergranular during the hold times. Clearly, hold times produced a sharp increase in crack growth rates, just as in the case of Astroloy, Fig. 7. An added feature of the hold time data recorded in Fig. 15 is the apparent retardation in crack growth immediately after resuming continuous cycling. Grain boundary cracks formed during the hold time periods, see Fig. 16, may have been responsible for relaxation of stresses at the crack tip prior to resumption of continuous cycling. Alternatively, a large plastic zone at the crack tip accompanying rapid crack growth could produce residual compressive stresses at the crack tip when continuous cycling resumed.

Low Cycle Fatigue

LCF data for Astroloy at 650°C and 725°C in argon are summarized in Fig. 17. A two min hold at peak strain is detrimental at each temperature, both in terms of total strain and plastic strain. A five min. hold at peak strain caused further degradation of LCF life. Note that the slopes of the plots of $\Delta\varepsilon_p$ vs. N_f remain constant with temperature and hold time; thus, the Coffin-Manson relation:

$$N_f^{\beta}\Delta\varepsilon_p = C \qquad (1)$$

is obeyed, with the constant slope suggesting that there is no change in fracture mechanism when a hold time is imposed. A summary of the terms β and C from Eq. 1 appears in Table III.

The beneficial effect of argon on LCF behavior may be seen in Fig. 18, which is a comparison of data from this investigation (in argon) with previous work carried out in air. Argon is beneficial at all cyclic strains, but the effect appears to be most marked at low cyclic strains.

Cyclic hardening was measured in Astroloy at each of the two test temperatures, as shown in Fig. 19. Note that there is virtually no effect of temperature on hardening in this range, and a linear relation between stress range (as saturation) and strain range is seen:

$$\left(\frac{\Delta\sigma}{2}\right)\text{MPa} = k\left(\frac{\Delta\varepsilon_p}{2}\right)^{n'}$$

For both temperatures $k \sim 2000$ and $n' \sim 0.1$.

Similar LCF experiments have been carried out on René 95, see Fig. 20, with Coffin-Manson slopes for continuous cycling recorded in Table IV. Again there is a detrimental effect of a hold time at peak strain when $\Delta\varepsilon_T$ is plotted against N_f.

For this alloy, plastic strain ranges were so small that they could not be measured accurately, especially at low total strain ranges. Therefore, no relation is shown between $\Delta\varepsilon_p$ and N_f.

However, very limited data for HIP René 95 in argon at 650°C from this investigation are compared to data for HIP and HIP + forged René 95 reported by others[2,3], see Fig. 21. There is little apparent effect of either atmosphere or microstructure on the results, all the data falling within a single scatter band.

The detrimental effects of hold times on René 95 in both air and argon may be noted in Fig. 22, which shows a more severe loss of life in argon. However, the hold time experiments in air were carried out on HIP + forged material, and it is not known to what extent the microstructure may have influenced that result.

Cyclic hardening of a sample of René 95 tested at 650°C is compared to data for Astroloy at the same total strain range (2%) in Fig. 23. Note that René 95 is the stronger alloy, so that the maximum stresses at each cycle are higher for René 95. However, the rate of cyclic hardening appears to be similar for both alloys.

Cyclic stress-strain curves for René 95 in two conditions (HIP, HIP + forged) and HIP Astroloy are compared in Fig. 24. Although René 95 appears to cyclically harden at a more rapid rate than Astroloy, it should be noted that the grain size of Astroloy (ASTM g.s. 5-7) is much larger than for René 95 (ASTM g.s. 11-14). The very rapid cyclic hardening of HIP + forged René 95 undoubtedly is a result of the excess dislocations imparted by the forging operation.

Fractographic examinations of the two alloys was carried out both to

determine the influence of hold times on crack path and to identify crack initiation sites such as second phase particles and inclusions. In the case of Astroloy, non-metallic inclusions rich in magnesium were responsible for crack initiation, see Fig. 25. These inclusions were typically 5-10μm in maximum dimension.

Striations were noted in many samples tested at 650°C and 725°C, and generally were brittle in appearance, see Fig. 26. Specimens subjected to a tensile hold had more readily visible striations at 650°C, as in Fig. 27; however, no striations were noted in hold time samples tested at 725°C, perhaps due to the presence of a substantial oxide film. The most notable feature of the hold time experiments was to produce a mixture of TG and IG cracking over most of the fracture surface compared to the TG fracture noted in samples subjected only to continuous cycling. A more notable effect of hold time was noted in the initiation zone, which was always TG for continuous cycling and IG for hold time samples. These results are summarized in Table V.

Cracks in René 95 were more likely to initiate at pores, as shown in Fig. 28a), for a sample tested at 725°C with no hold time, and in Fig. 28b) for a specimen tested at 650°C with a 2 min. hold. In one sample, tested at 650°C with $\Delta\varepsilon_t$=1.54%, both particles and pores were responsible for crack initiation. Results of all fractographic observations on René 95 are summarized in Table VI. With no hold time, both initiation and propagation were TG. However, with a hold time initiation was IG and propagation was IG + TG. Therefore, the effects of a hold time on crack path are very similar in the two alloys. Striations were seen in a few continuously cycled specimens of René 95, but were not observed in samples subjected to a hold time.

DISCUSSION

A major aim of this investigation was to determine the relative importance of creep and environmental interaction of fatigue behavior of the test alloys. The constant stress hold at peak load is meant to simulate a creep dwell, as may be experienced by the rim at blade attachment areas. During LCF testing, tests in vacuum led to excessive heating of the extensometer. For ease of comparison of da/dN and LCF results it was decided, therefore, to run both crack growth and LCF tests in argon. The crack growth tests showed that argon is intermediate between air and a relatively poor vacuum (10^{-4} to 10^{-5} torr) in its effect on crack growth rates (see Fig. 6 for Astroloy and Fig. 9 for René 95).

To describe the FCG behavior of the two alloys, the Paris equation

$$\frac{da}{dN} = A\ (\Delta K)^m \qquad (1)$$

may be used. The constants found for different conditions are listed in Table VII.

The magnitude of the exponent and the pre-exponential factor were higher in air and in hold time tests than those in argon. The slopes for René 95 were somewhat lower than those for Astroloy under similar test conditions.

This equation can be used for life prediction. However, it should be noted that most of the René 95 specimens showed large overload regions as opposed to Astroloy. This in turn means that the limiting crack length (a_f) prior to catastrophic failure is smaller for René 95. Hence in spite of lower slopes, René 95 shows decreased total life.

The separation of $\frac{da}{dN}$ into individual fatigue, creep or oxidation fractions, if, and to find the fractional contribution of each as suggested by Wei et al[14], was not possible because appreciable oxidation occurred even in argon. On the basis of our observations, it can be suggested that the superposition model

for Astroloy and René 95 at 650°C in argon reduces to:

$$\frac{da}{dN} = f_{\text{fatigue}} \times \left(\frac{da}{dN}\right)_{\text{fatigue}} + f_{\text{oxide}} \times \left(\frac{da}{dN}\right)_{\text{oxide}} \qquad (2)$$

since creep damage was insignificant.

As a consequence of the lack of parametric data such as strain rate sensitivity, other models such as the modified damage model[15] or strain rate dependent models,[16] could not be applied at this stage.

The oxide film produced in argon has been measured by Scanning Auger Spectroscopy. The results show a chromium-rich oxide (whether CrO_3 or Cr_2O_3 could not be established) about 2000Å thick is formed after a test at 650°C. It appears that oxidation played a major role in decreasing fatigue life or increasing crack growth rate under conditions of lower test frequency or a hold time at peak load. Little or no evidence for creep damage under hold time conditions could be found.

The increased crack growth rate and reduced life associated with hold time experiments can be related to the change in crack origin from TG to IG (LCF) and the crack path to mixed TG and IG.

The behavior of air in promoting crack growth has been related in the past to oxygen diffusion down grain boundaries, as well as localized oxidation damage at the crack tip.[4-9] Oxide growth stresses at the crack tip may also promote crack growth.[10] In the present work, although unmistakable evidence of oxidation during crack growth in argon was observed, the crack path remained transgranular in both FCG and LCF experiments, except when tensile holds were imposed. Increased TG crack growth in argon relative to vacuum could arise from accelerated diffusion of oxygen into slip planes, although no direct evidence for such a mechanism was observed.

It is difficult to explain why temperature had so little effect on crack growth or fatigue life, especially between 650°C and 725°C. Whether creep damage or oxidation contributed to the rate of fatigue crack growth at 650°C, increasing the temperature to 725°C should have produced a significant rise in FCG and LCF life degradation. This did not occur for Astroloy, as shown in Figs. 4 and 17, respectively. Insufficient data have been obtained for René 95 to determine whether t' erature insensitivity is observed in that alloy.

Very different sensitivities to oxygen have been demonstrated between γ'-strengthened nickel base superalloys. For example, Sadananda and Shahinian[11] have shown that although FCG rates are the same in IN718 and PE16 in vacuum, rates are increased in air by a factor of two for PE16 but more than a factor of ten for 718. Similarly, a 1 min. hold in air had no effect on PE16 but a 100X increase in FCG was observed in IN718. A similar increase in FCG rate (100X) was observed in the present work for both Astroloy and René 95 in argon when a 2 min. hold was imposed. The extreme sensitivity of crack growth rates of René 95 and Astroloy to decreasing frequency and to hold times in air or in argon is probably therefore, a manifestation primarily of the susceptibility of these alloys to oxygen induced damage. The most noteworthy feature of the fracture mechanism in these alloys, however, is the maintenance of a TG crack path, both in FCG and LCF experiments, even at low frequencies.

Recent theories of creep cavitation in Ni-base alloys are based on internal gas bubble formation, typically CO or CO_2[12,13] and the gas pressure is assumed as the major driving force for cavity nucleation. Our calculations for these alloys indicate that the gas pressures at 650°C would be at most of the order of 5-14 Pa. Obviously such low pressures cannot nucleate the cavities. This partially explains why insignificant creep damage was observed.

It is interesting to compare the results of our hold-time experiments on HIP René 95 with data previously reported by AFML for cast and wrought René 95. Tests were conducted on the latter material at 650°C with one and ten min. hold periods in tension and compression. Our own two min. hold time tests in argon on HIP material provided precisely the same lives, based on total strain, as those noted on the cast and wrought alloy. The earlier work showed that tensile holds were not very damaging, and that, in fact, compressive hold periods were much more damaging. For cast René 80, tensile holds were actually reported to be beneficial relative to continuous cycling. Lord and Coffin[19] suggested that those unusual results might be explained if, during a tensile hold, compressive mean stresses are introduced while in compressive holds a tensile mean stress develops as hysteresis loops stabilize. Tensile mean stresses should degrade LCF resistance, while compressive mean stresses should prolong life.

In our own work, conducted in argon, no such beneficial effect of tensile holds was noted in either alloy, whether in load controlled FCG or strain-controlled LCF experiments, especially when the latter data were plotted as plastic strain vs N_f. For example, life of HIP René 95 was reduced from 2600 cycles to 200 cycles at $\Delta\varepsilon_p=4\times10^{-4}$. In the case of Astroloy, a distinct loss of life with tensile holds was noted whether data were plotted against $\Delta\varepsilon_t$ or $\Delta\varepsilon_p$, see Fig. 17. However, the effect was more readily apparent on the basis of $\Delta\varepsilon_p$, and clearly a 5 min. hold was more damaging than a two min. hold.

Before examining these apparently contradictory results in more detail, it must be emphasized that the previous work on cast and wrought René 95 and René 80 was carried out in air, under diametral strain control. (The method of strain control is not considered to be significant). Our own experiments in

argon permitted some oxidation to occur, but clearly at a lower rate than would be the case in air. Load-controlled FCG experiments with a 2 min. hold, conducted in our laboratory, have shown that cracks do not propagate readily in air in either alloy. In order to maintain crack extension, the load periodically has to be increased. This observation suggests that crack blunting, caused by extensive oxide buildup at the crack tip during the hold periods, can slow or even stop crack growth. We suggest, then, that oxygen, while clearly embrittling to these alloys at relatively low concentrations, can effectively supress crack growth when present at the usual levels in air. Therefore, we conclude that the response of superalloys to tensile and compressive hold periods will depend sensitively upon the oxygen pressure, and that either beneficial or detrimental effects of such holds may be expected, depending upon environmental conditions.

REFERENCES

1. H. Tada, P.C. Paris and G.R. Irwin, "The Stress Analysis of Cracks Handbook", Del Research Corp. Hellertown, PA, 1973.

2. S. Bashir, P. Taupin and S.D. Antolovich, Met. Trans. A, 1979, V 10A, p. 1481.

3. B.A. Cowles, J.R. Warren and F.K. Haake, "Evaluations of Cyclic Behavior of Aircraft Turbine Disk Alloys", P & WA Technical Report for NASA CR-165123 (1980).

4. M.L. Sessions, C.J. McMahon and J. Walker, Mat. Sci. & Eng., 1977, V 27, p. 17.

5. P.N. Chabu and C.J. McMahon, Met. Trans. A, 1974, V 5, p. 441.

6. M.N. Menon, J. Mat. Sci., 1976, V 11, p. 984.

7. J.C. Runkle and R.M. Pelloux, in "Fatigue Mechanisms", STP 675, ASTM, 1979, p. 501.

8. J. Wareing, Met. Trans. A, 1977, V 8, p. 711.

9. D.A. Woodford, Met. Trans. A, 1981, V 12, p. 299.

10. S. Floreen and R.H. Kane, Met. Trans. A, 1979, V 10, p. 1745.

11. K. Sadananda and P. Shahinian, Metals Technology, Jan. 1982, p. 18.

12. K. Raj, Acta Met., 1982, V 30, p. 1259.

13. B. F. Dyson, Acta Met., 1982, V 30, p. 1639.

14. R.P. Wei and G.W. Simmons, "Recent Progress in Understanding Environmentally Assisted FCG" Technical Rep. #8, ONR N00014-C-0543, NR036-097, Jan. 1979.

15. D.A. Jablonski, and R.M.N. Pelloux, Met. Trans. A, V 8A, 1977, p. 1893.

16. P.S. Maiya and S. Majumdar, Met. Trans. A, V 8A, 1977, p. 1651.

17. D.A. Cowles, J.R. Warren and F.K. Haake, "Evaluations of Cyclic Behavior of Aircraft Turbine Disk Alloys", NASA NAS 3-20367 (quoted from P & WA Technical Report for NASA CR-165123 (1980), p. 70).

18. Life Prediction Techniques for Analyzing Creep-Fatigue Interactions in Advanced Nickel Base Superalloys, Wright State Univ., July 1976 (quoted in L.F. Coffin, Jr. in Fatigue Environment and Temperature Effect, J.J. Burke and V. Weiss, Eds., Plenum Press, New York 1983).

19. D.C. Lord and L.F. Coffin, Jr., Met. Trans. V 4, 1973, p. 1657.

TABLE I

Chemical Composition

	C	Cr	Co	Mo	Cb	Zr	Ti	Al	W	B	Ni
HIP-Astroloy*	0.02	15.1	17	5.2	-	<.01	3.5	4	<.05	.025	Bal.
HIP-René 95**	0.05	13	8.3	3.5	3.5	.04	2.5	3.6	3.4	-	Bal.

Mechanical Properties

	UTS MPa	0.2%σ_y MPa	%El	%RA	T
HIP-Astroloy	1393	936	26	31	Room T.
	1287	869	26	28	538°C
HIP-René 95	1936	1214	16	15	Room T.
	1514	1119	16	17	650°C

Microstructure

HIP-Astroloy γ-γ' - $M_{23}C_6$ MC
volume fraction of γ' = 42% grain size: 40-60μm

René 95 γ-γ' - $M_{23}C_6$ MC
volume fraction of γ' = 48% grain size: 10-15μm with occasional 40μm large grains

* Supplied by Pratt and Whitney - NASA

** Supplied by G. E. - NASA

TABLE II

Test matrix to be followed for each alloy

R = 0.05 ν: frequency in Hz

	575°C	650°C	725°C
1. Argon, Hold time = 0			
ν = 0.33		*	
ν = 1	*	*	*
ν = 20	*	*	*
2. Air, Hold time = 0			
ν = 0.33		*	
ν = 1	*	*	*
ν = 20	*	*	*
3. Argon, Hold time tests with ν = 1 Hz			
Hold time = 120 s		**	**
Hold time = 360 s		**	
4. Air, Hold time tests with ν = 1 Hz			
Hold time = 120 s		**	
Hold time = 360 s		**	

* waveform 

** waveform 

TABLE III

Coffin-Manson Constants for Astroloy

$\Delta\epsilon_p N_f^{\beta} = C.$

	β	C
650°C, 0 hold	0.96	1.11
725°C, 0 hold	0.91	0.6
650°C, 2 min hold	0.94	0.3
725°C, 2 min hold	0.99	0.4
650°C, 5 min hold	0.96	0.2

TABLE IV

Coffin-Manson Constants for René 95

650°C, 0 hold	0.72	0.13
725°C, 0 hold	0.73	0.11

TABLE V

Summary of Fractographic Studies of HIP Astroloy

$\Delta\varepsilon_t$(%)	$\Delta\varepsilon_p$(%)	Type Test	N_f	Initiation	Propagation	Comments on Origin
1.56	0.065	650°C 0 hold	2321	TG	TG	flat striations
2.03	0.3	650°C 0 hold	484	TG	TG	flat striations
2.57	0.55	650°C 0 hold	250	TG	TG + void	slightly rough striations
1.59	0.087	725°C 0 hold	1377	TG	TG	flat, striations
1.98	0.32	725°C 0 hold	307	TG	TG	slightly rough, striations
2.62	0.59	725°C 0 hold	173	TG	TG + void	slightly rough, striations
1.67	0.07	650°C 2 min hold	945	IG	TG + IG	no dimples striations
2.66	0.78	650°C 2 min hold	74	IG	TG + IG	some dimples no striations
2.05	0.25	725°C 2 min hold	62	IG	TG + IG	GB cracking many dimples, no striations
2.37	0.89	725°C 2 min hold	20	IG	TG + IG	GB cracking many dimples, no striations
1.5	0.076	650°C 5 min hold	358	IG	TG + IG	no striations
2.08	0.268	650°C 5 min hold	118	IG	TG + IG	GB cracking no striations
2.635	0.968	850°C 5 min hold	26	IG	TG + IG	GB cracking no striations

All have multiple origins associated with particles.

HIP Astroloy: ASTM grain size 5 - 7 grain dia. = 40 - 60μm

TABLE VI

Summary of Fractographic Studies of HIP René 95

$\Delta\varepsilon_t$(%)	$\Delta\varepsilon_p$(%)	Type Test	N_f	Initiation	Propagation	Comments on Origin
1.54	0.045	650°C 0 hold	2702	TG	TG	particles, pore, no striations
2.04	0.12	650°C 0 hold	498	TG	TG	particle, striations
2.56	0.32	650°C 0 hold	191	TG	TG	no striations
1.52	0.105	725°C 0 hold	570	TG	TG	pore no striations
2.08	0.33	725°C 0 hold	203	TG	TG	pore striations
2.61	0.36	725°C 0 hold	105	TG	TG	pore no striations
1.68	0.039	650°C 2 min hold	224	IG	TG + IG	no striations
2.05	0.2	650°C 2 min hold	135	IG	TG + IG	pore no striations
2.70	0.39	650°C 2 min hold	10	IG	TG + IG	pore no striations
1.66	0.096	725°C 2 min hold	122	IG	TG + IG	no striations
2.04	0.2	725°C 2 min hold	39	IG	TG + IG	no striations

Striations are generally not observed.

All have multiple origins associated with surface connected particles or pores.

HIP René 95: grain size 5 - 40μm(non-uniform)

TABLE VII

Constants of the Paris Equation for FCG at 650°C

	Astroloy		René 95	
	A	m	A	m
Argon				
0.33Hz			1.51×10^{-11}	3.1
1Hz	3.38×10^{-13}	4.1	6.30×10^{-9}	1.2
20Hz	5.01×10^{-13}	3.7	1.99×10^{-10}	1.9
2m hold	4.46×10^{-14}	5.6 (725°C)	2.45×10^{-9}	2.8
Air				
1Hz	1.38×10^{-12}	4.0	1.15×10^{-9}	1.9
20Hz	2.24×10^{-13}	4.3	8.71×10^{-11}	2.5

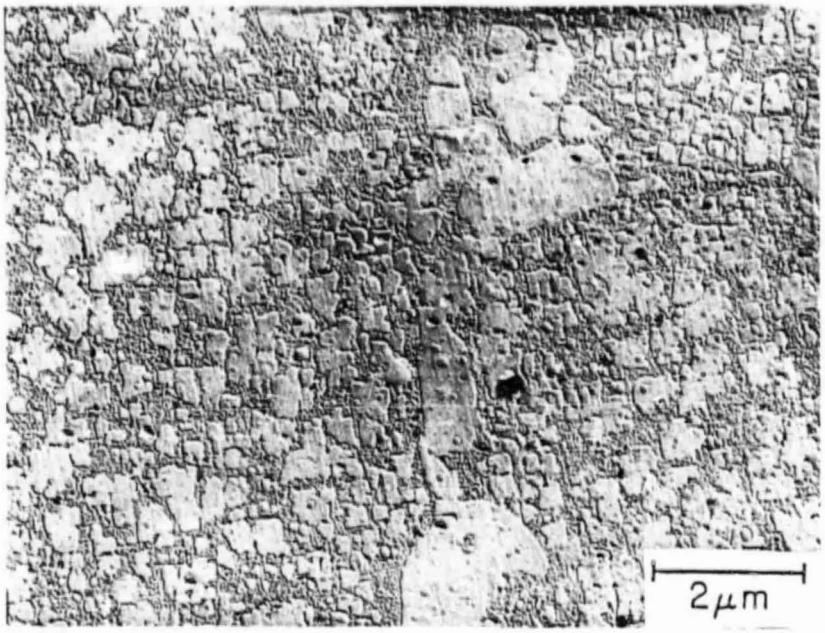

a) low magnification

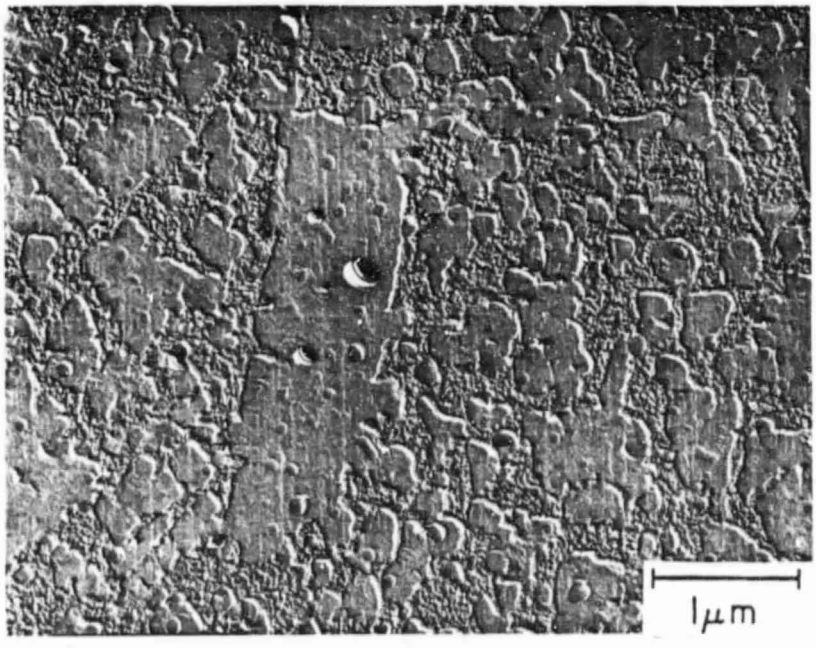

b) high magnification

Fig. 1 Transmission electron micrograph of Astroloy, plastic replica

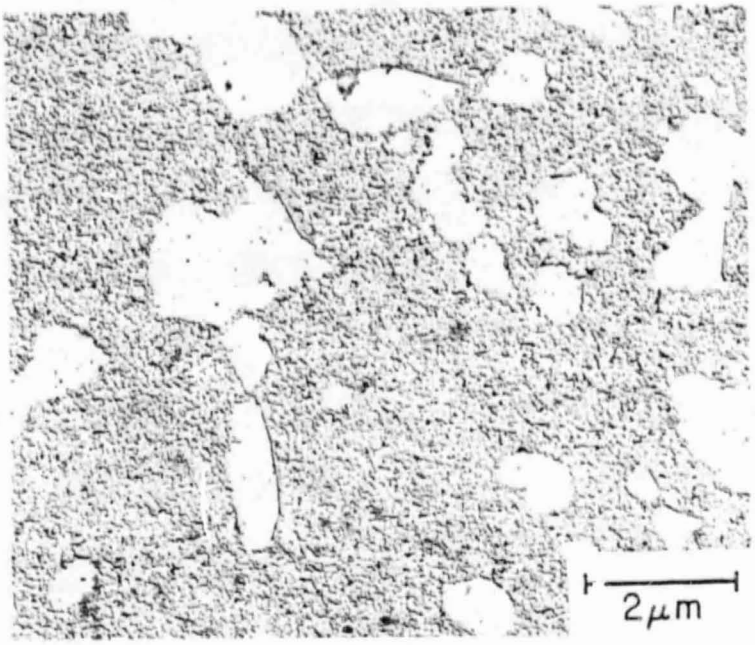

a) low magnification

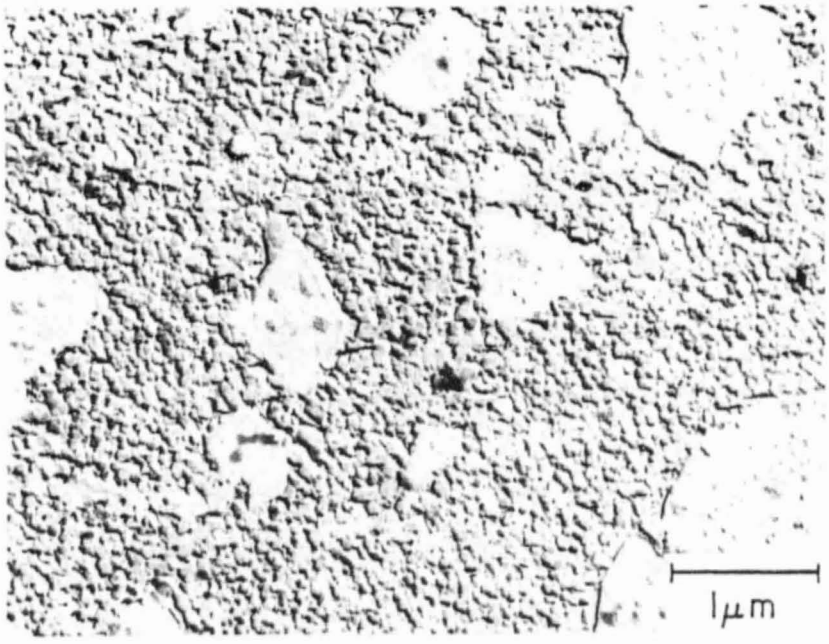

b) high magnification

Fig. 2 Transmission electron micrograph of René 95, plastic replica

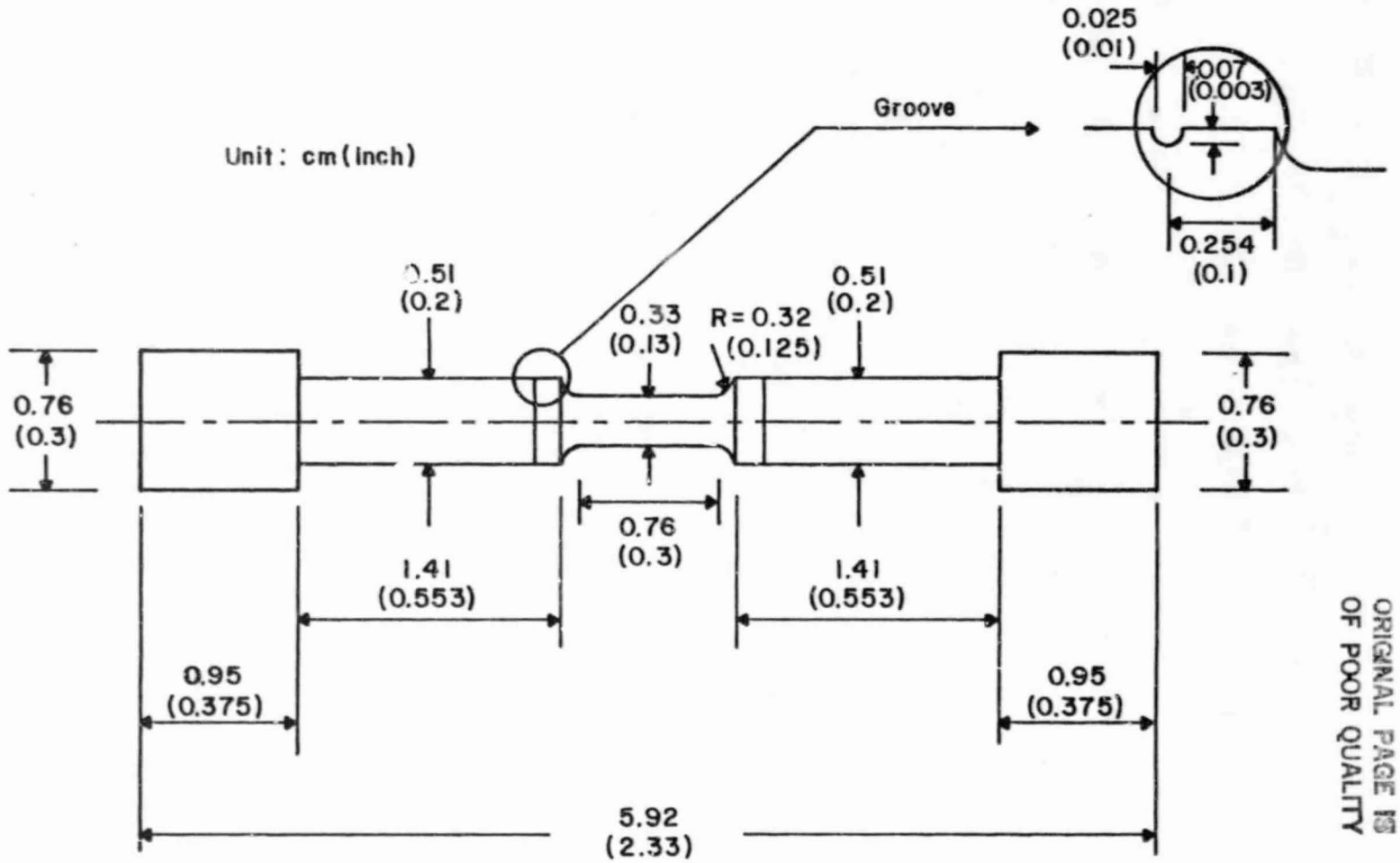

Fig. 3 Low cycle fatigue specimen design

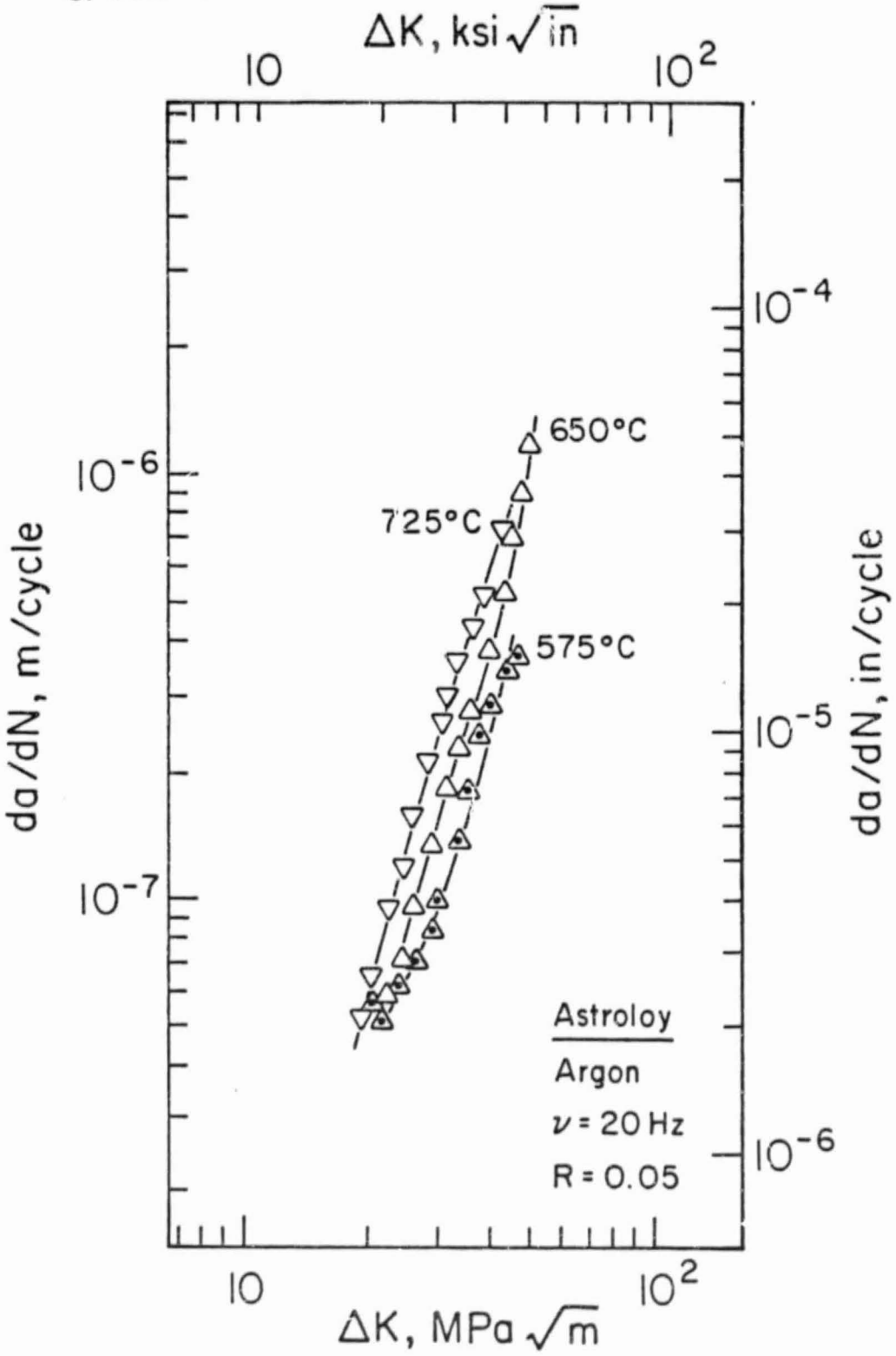

Fig. 4 Effect of temperature on FCG in Astroloy

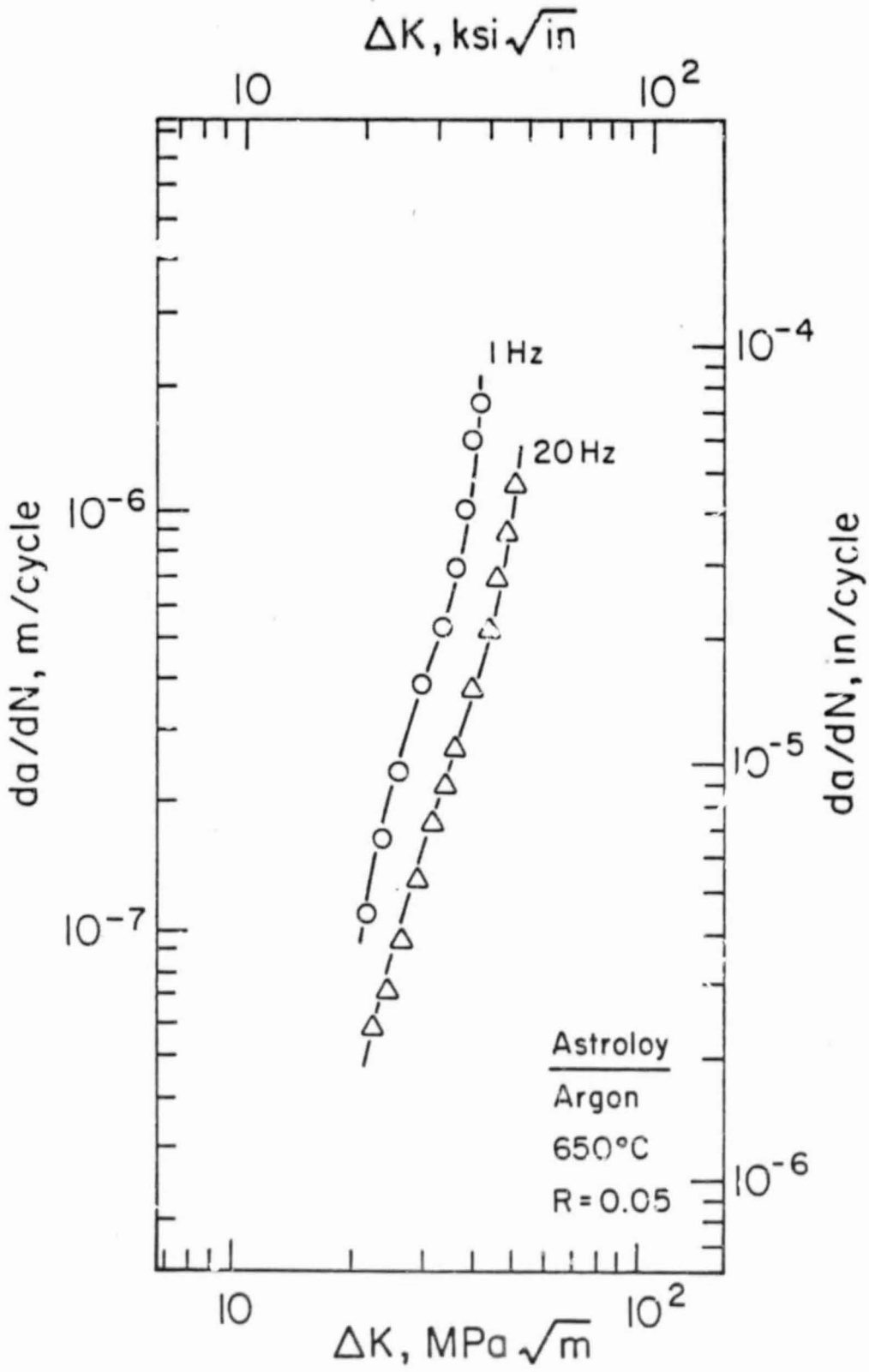

Fig. 5 Effect of frequency on FCG in Astroloy

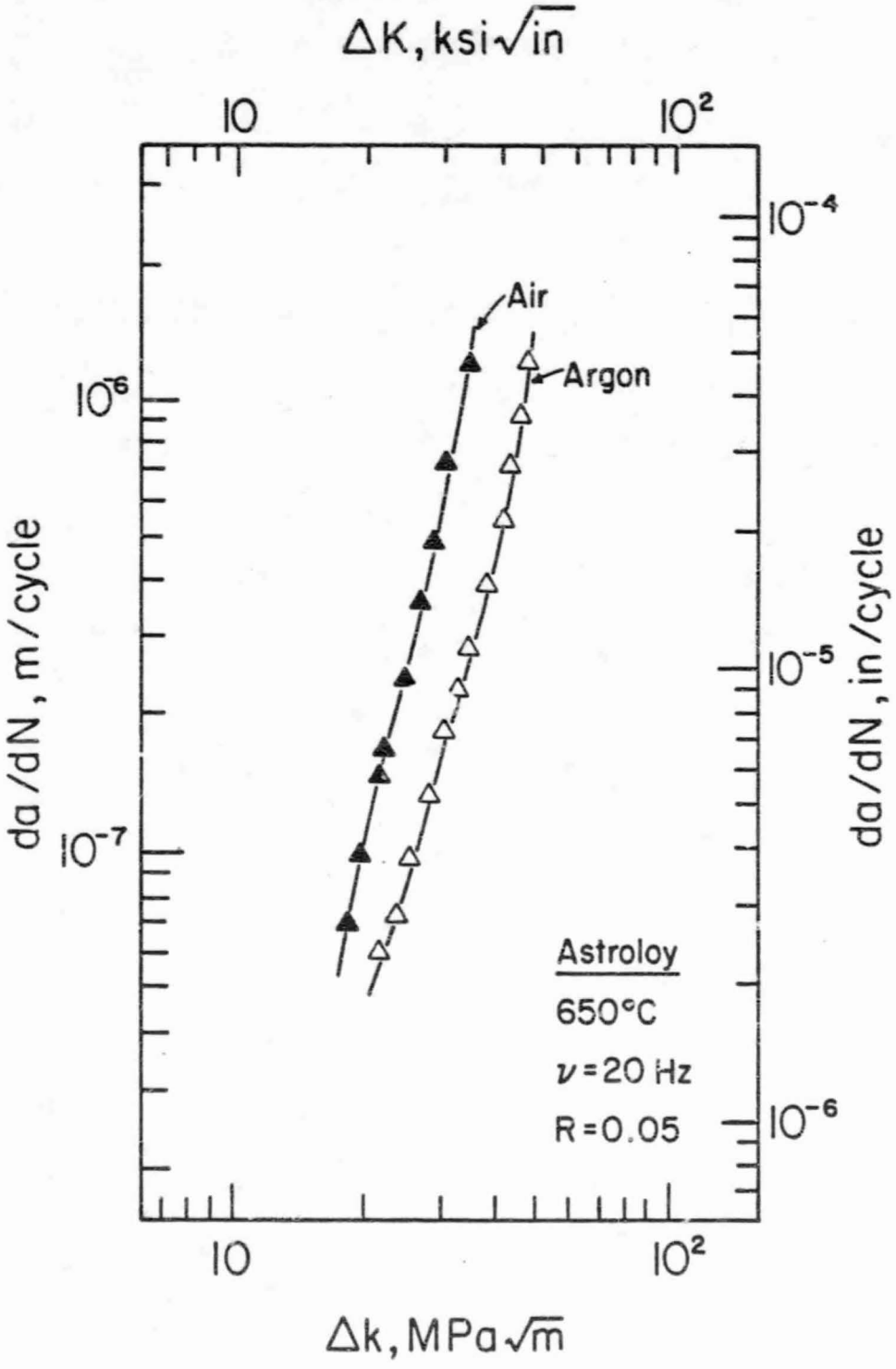

Fig. 6 Effect of environment on FCG of Astroloy

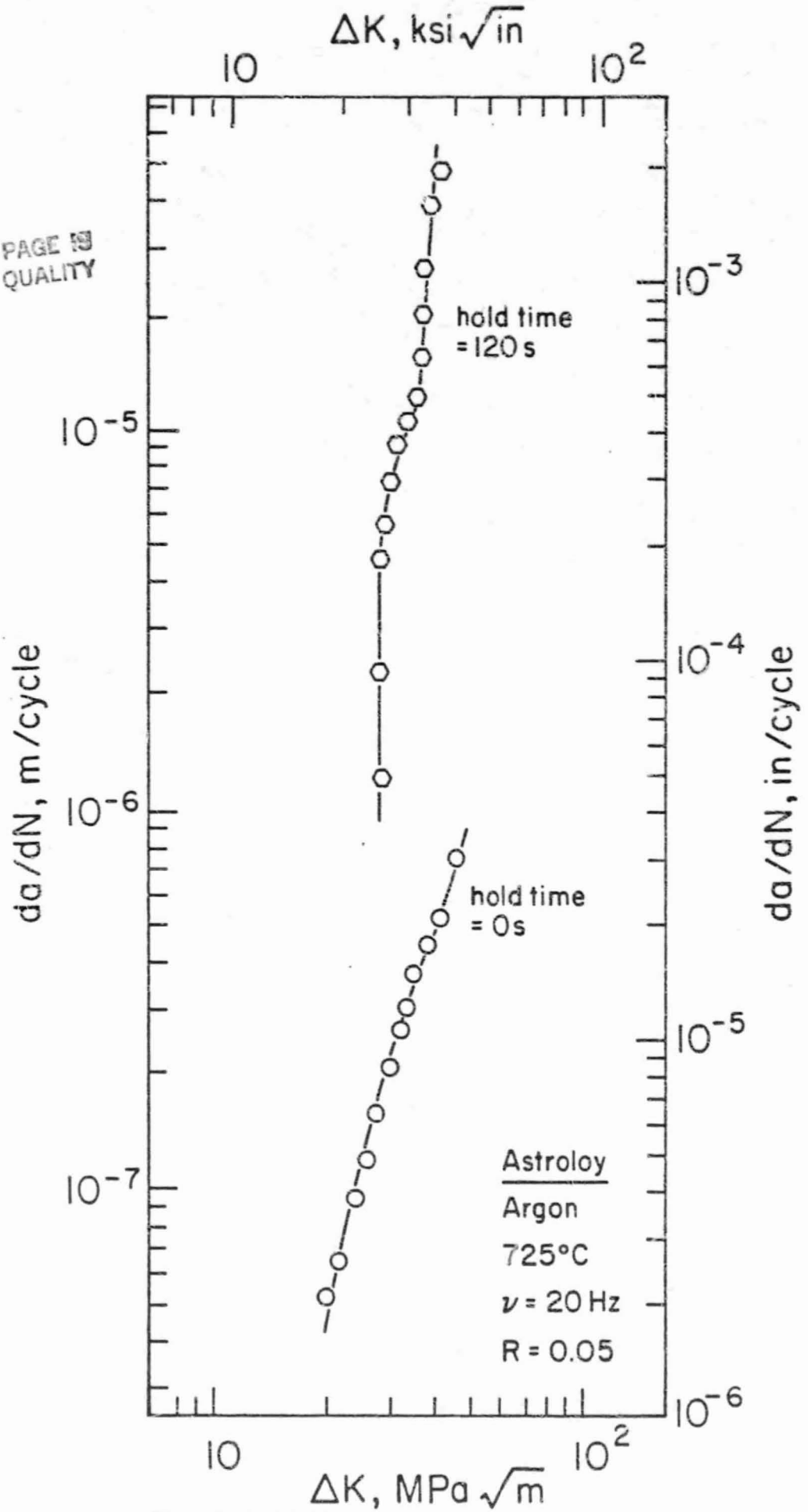

Fig. 7 Hold time effect on FCG of Astroloy

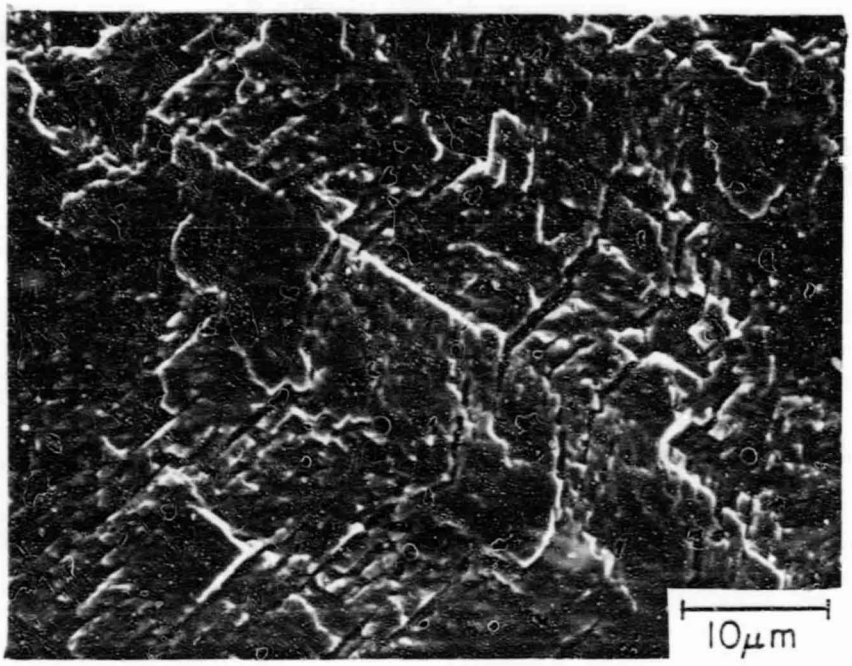

a) 25°C

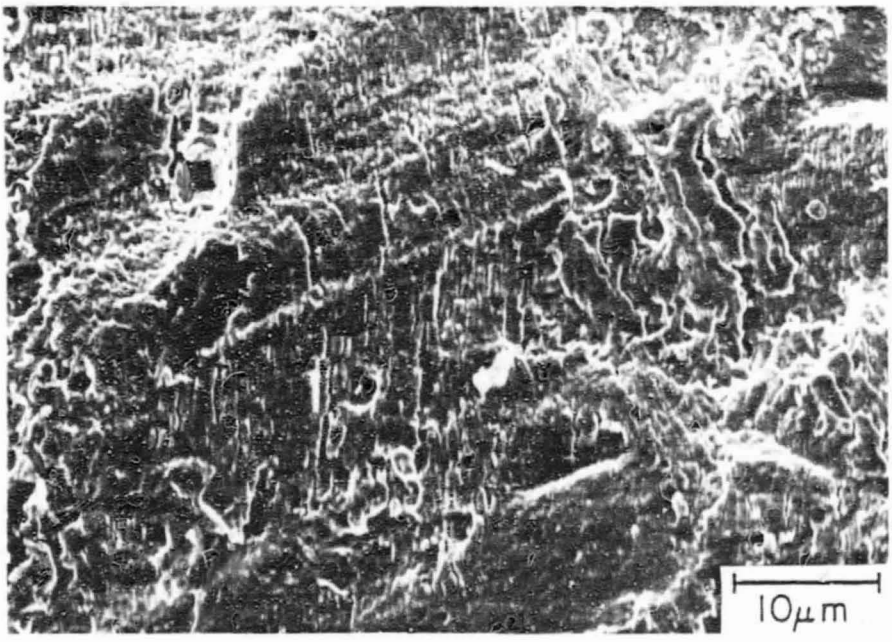

b) 650°C

Fig. 8 Brittle striations in Astroloy, air, ν=20Hz

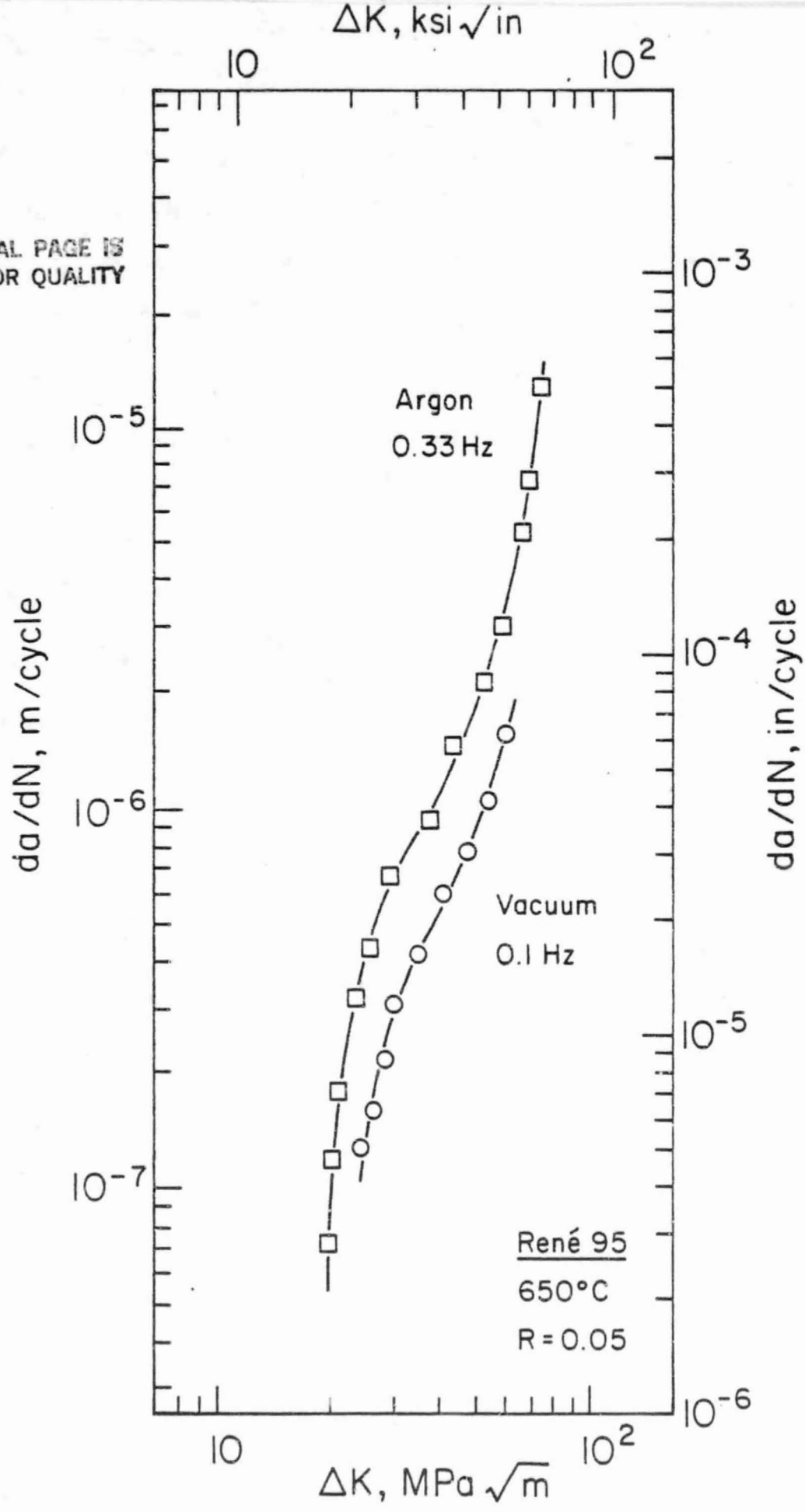

Fig. 9 Effects of environment on FCG of René 95

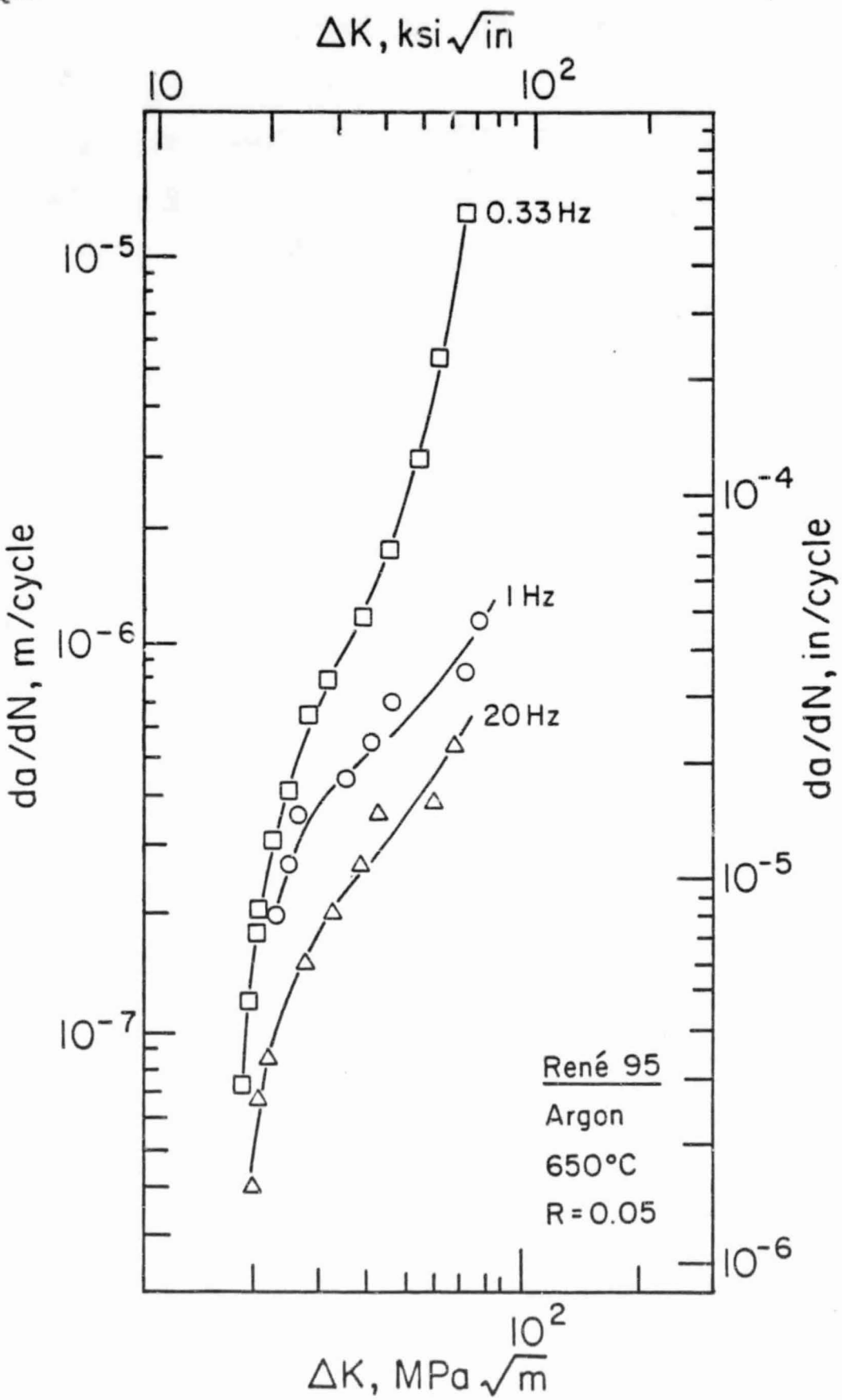

Fig. 10 Effect of frequency on FCG of René 95

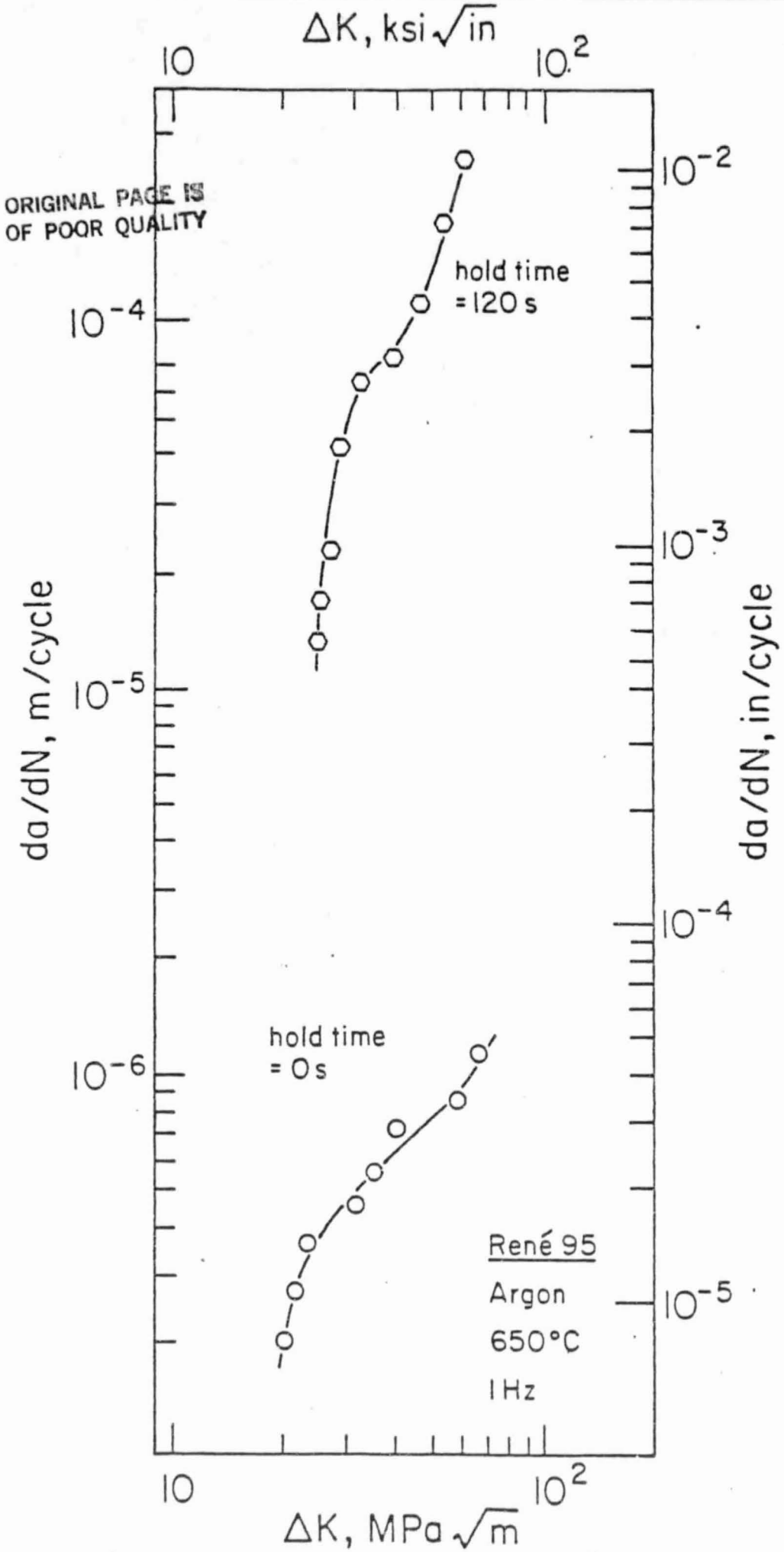

Fig. 11 Hold time effect on FCG of René 95

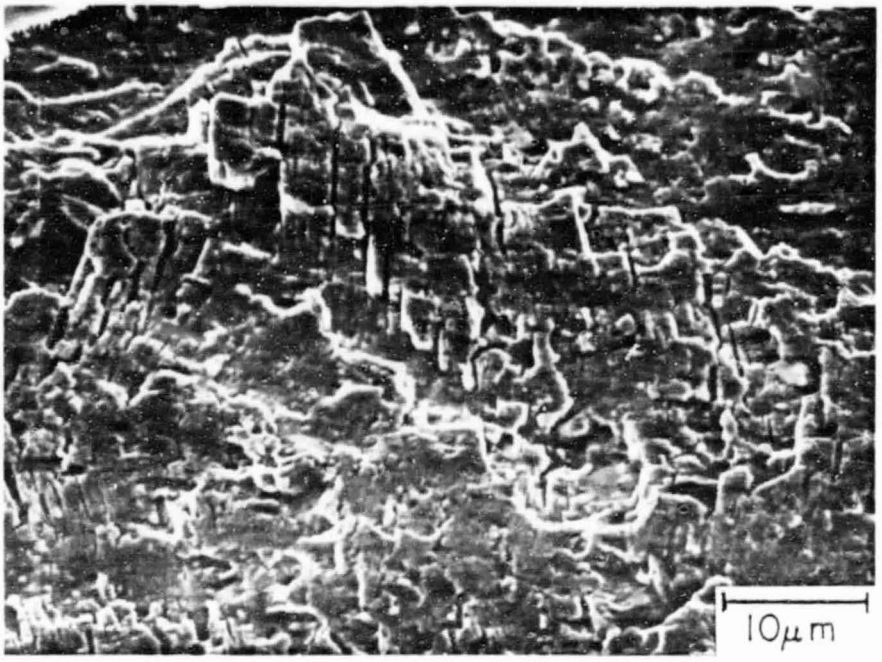

Fig. 12 SEM fractograph of brittle striations in René 95, 650°C, argon, 1Hz

650°C

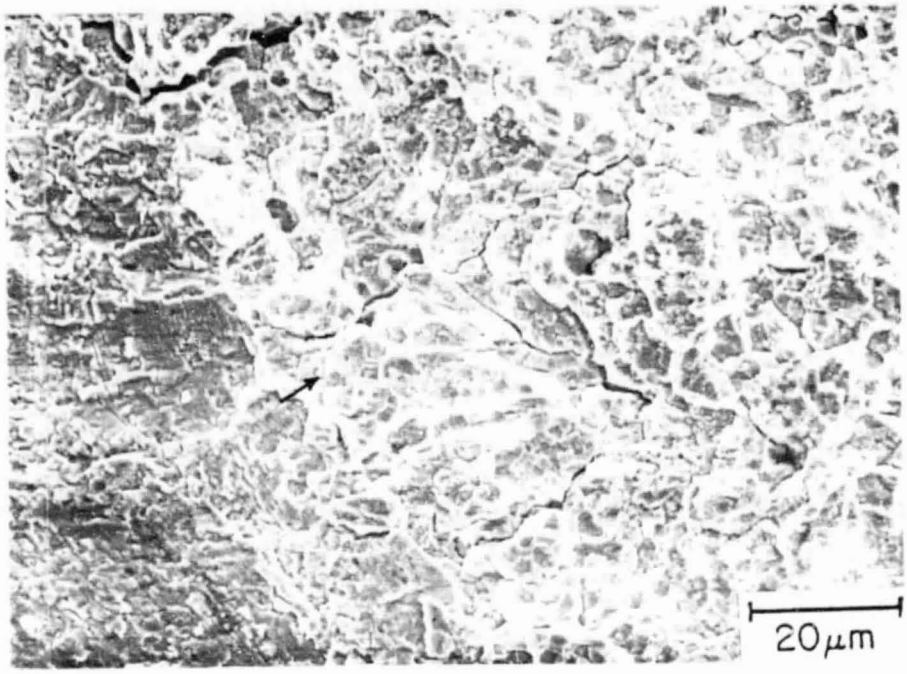

25°C

Fig. 13 Fracture surface in region of precrack-crack transition, René 95, argon, hold time = 120 s (1Hz)

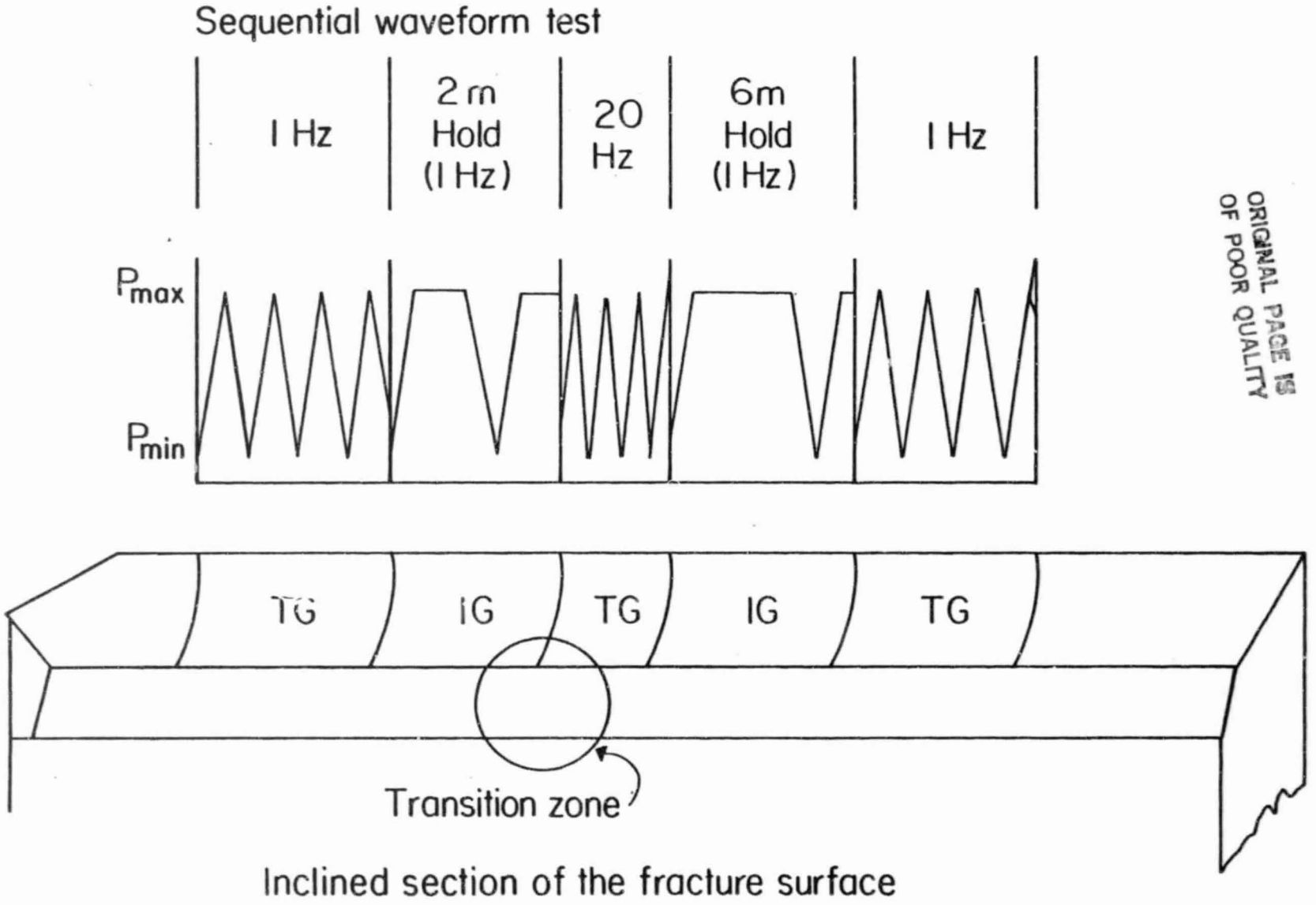

Fig. 14 Schematic diagram of sequential loading experiments

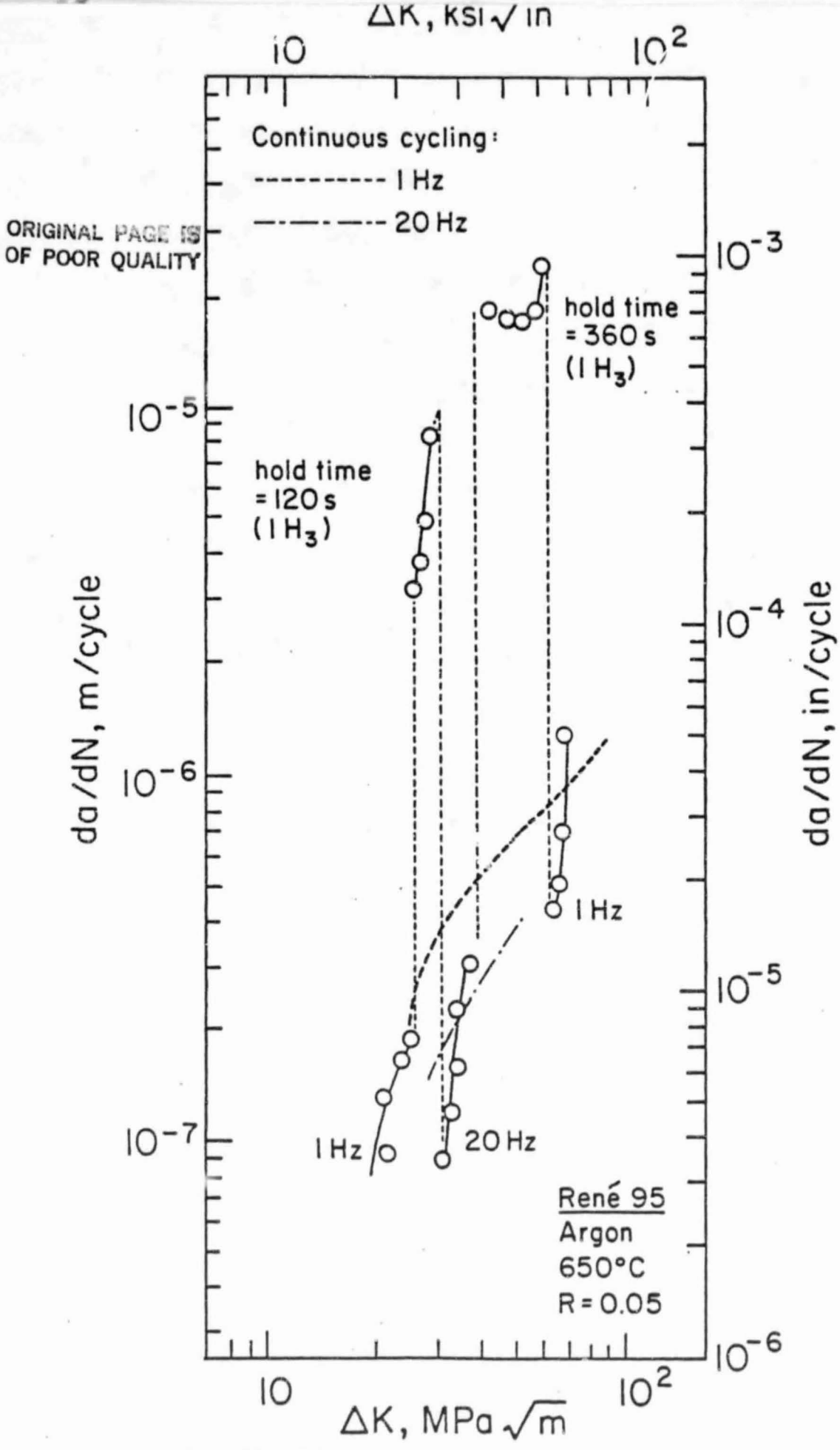

Fig. 15 Effects of sequential loading on FCG in René 95

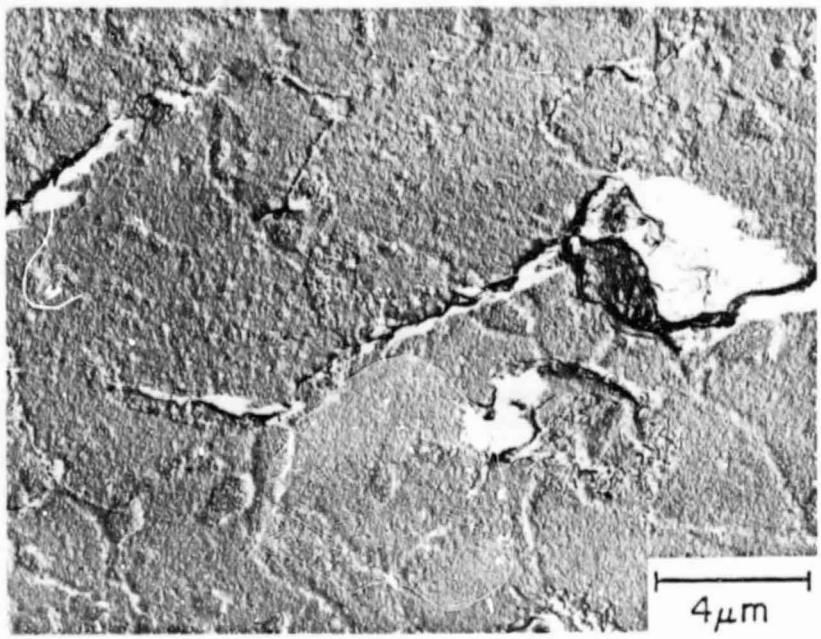

Fig. 16 Grain boundary damage in René 95, 650°C, argon, hold time = 360 s (1Hz). Plastic replica of the side surface

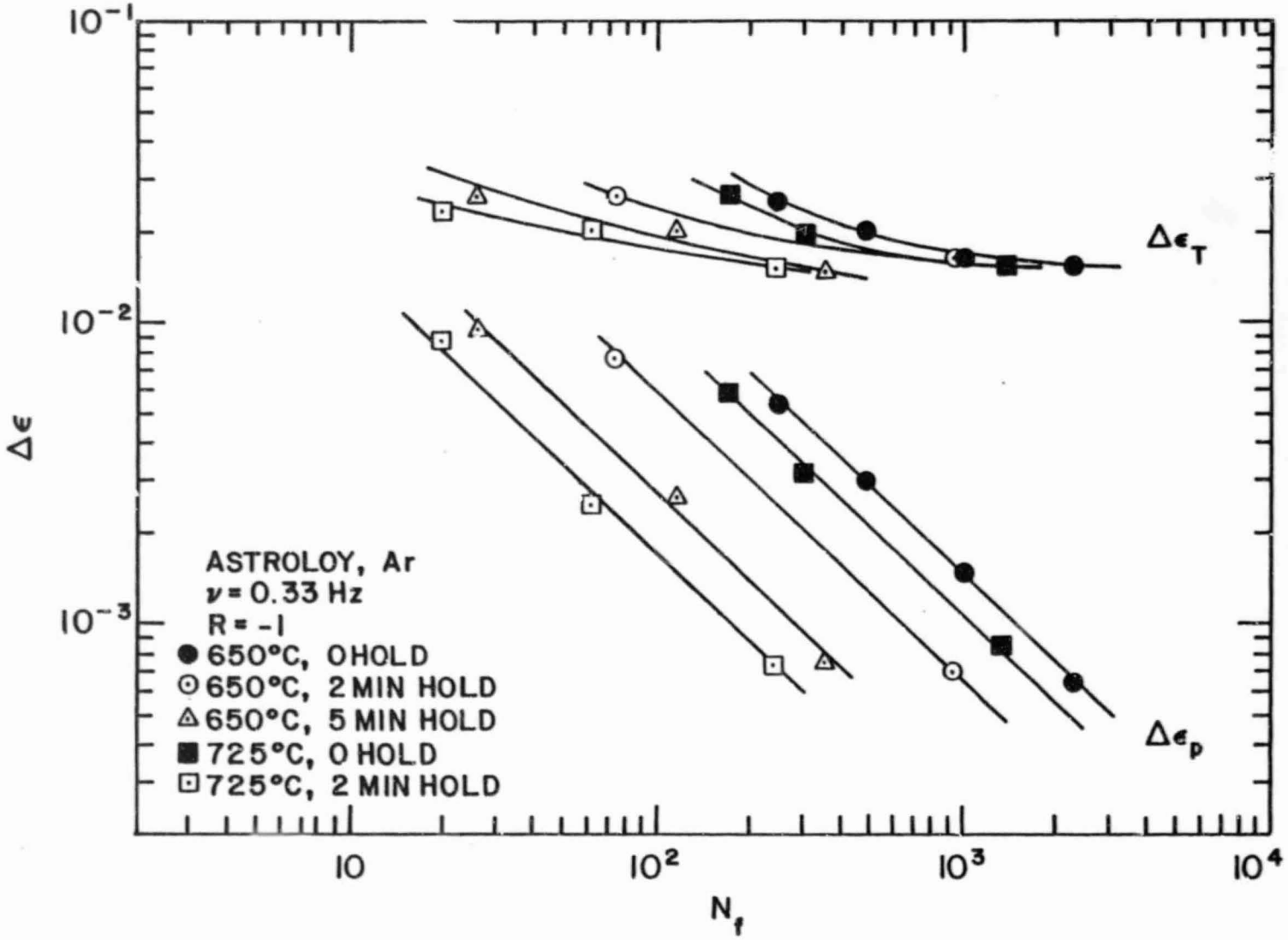

Fig. 17 LCF data for Astroloy

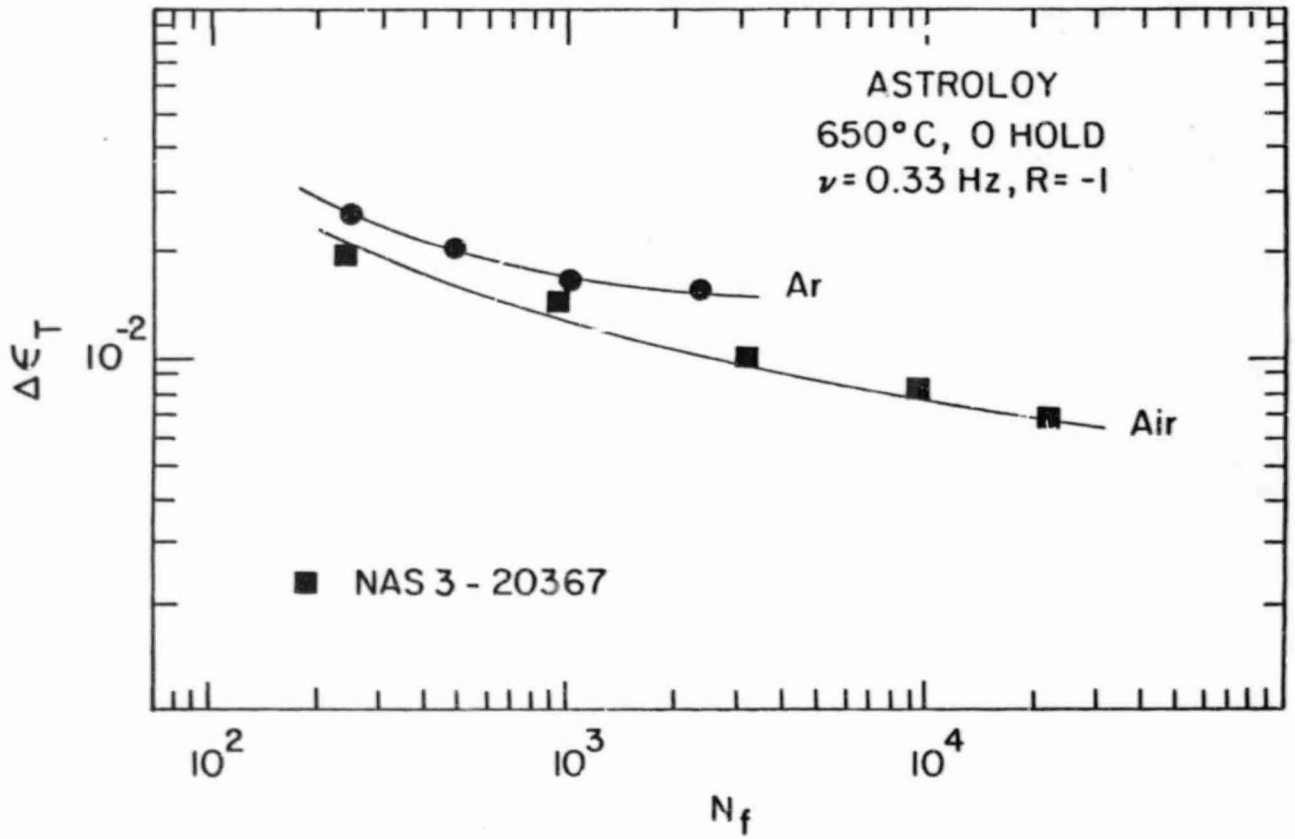

Fig. 18 Effect of environment on LCF of Astroloy.
Data in air from Ref. 17

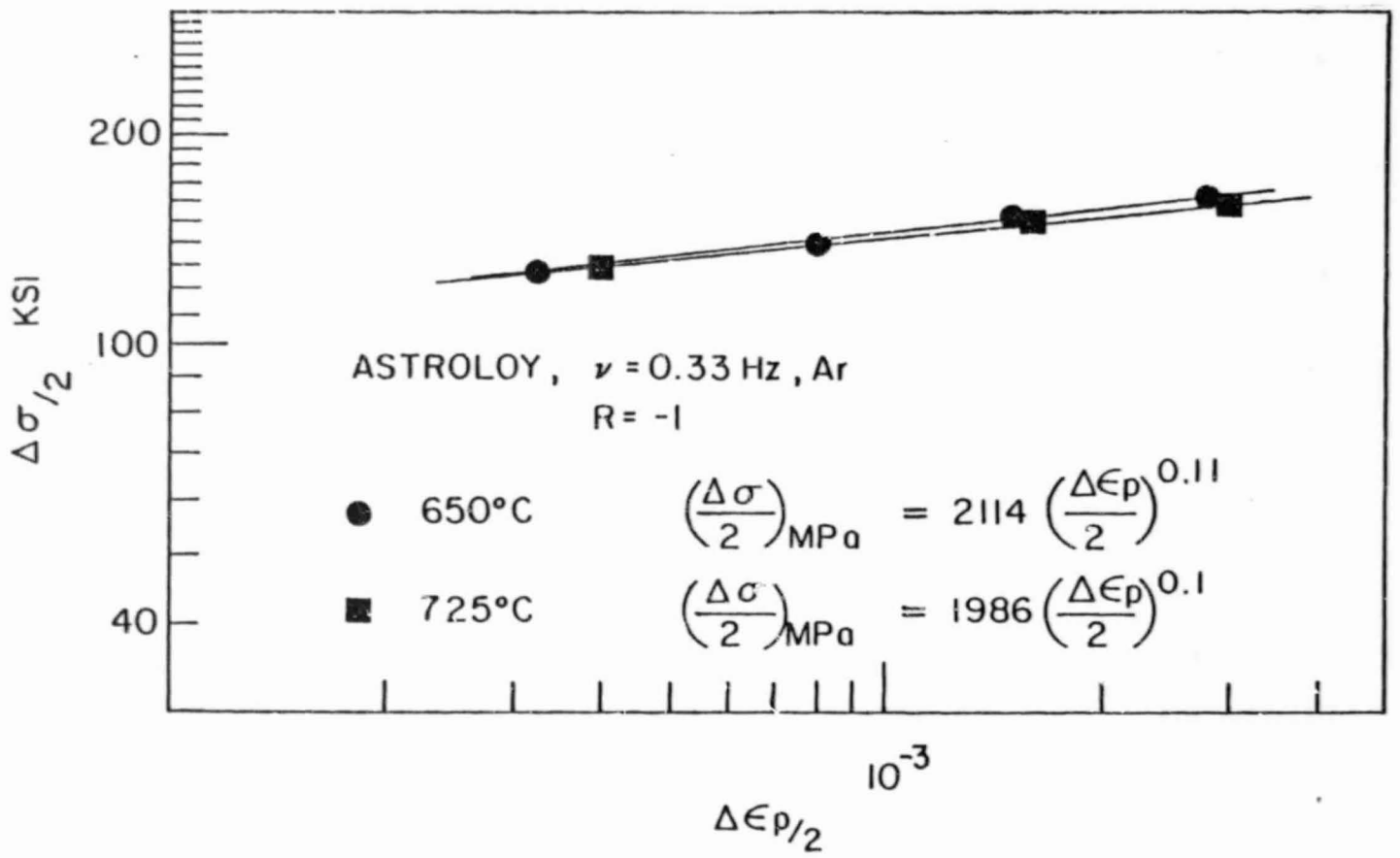

Fig. 19 Effect of temperature on cyclic stress-strain curve for HIP Astroloy ($^{\Delta\sigma}/_2$ and $^{\Delta\varepsilon}p/_2$ are measured at $^{N}f/_2$)

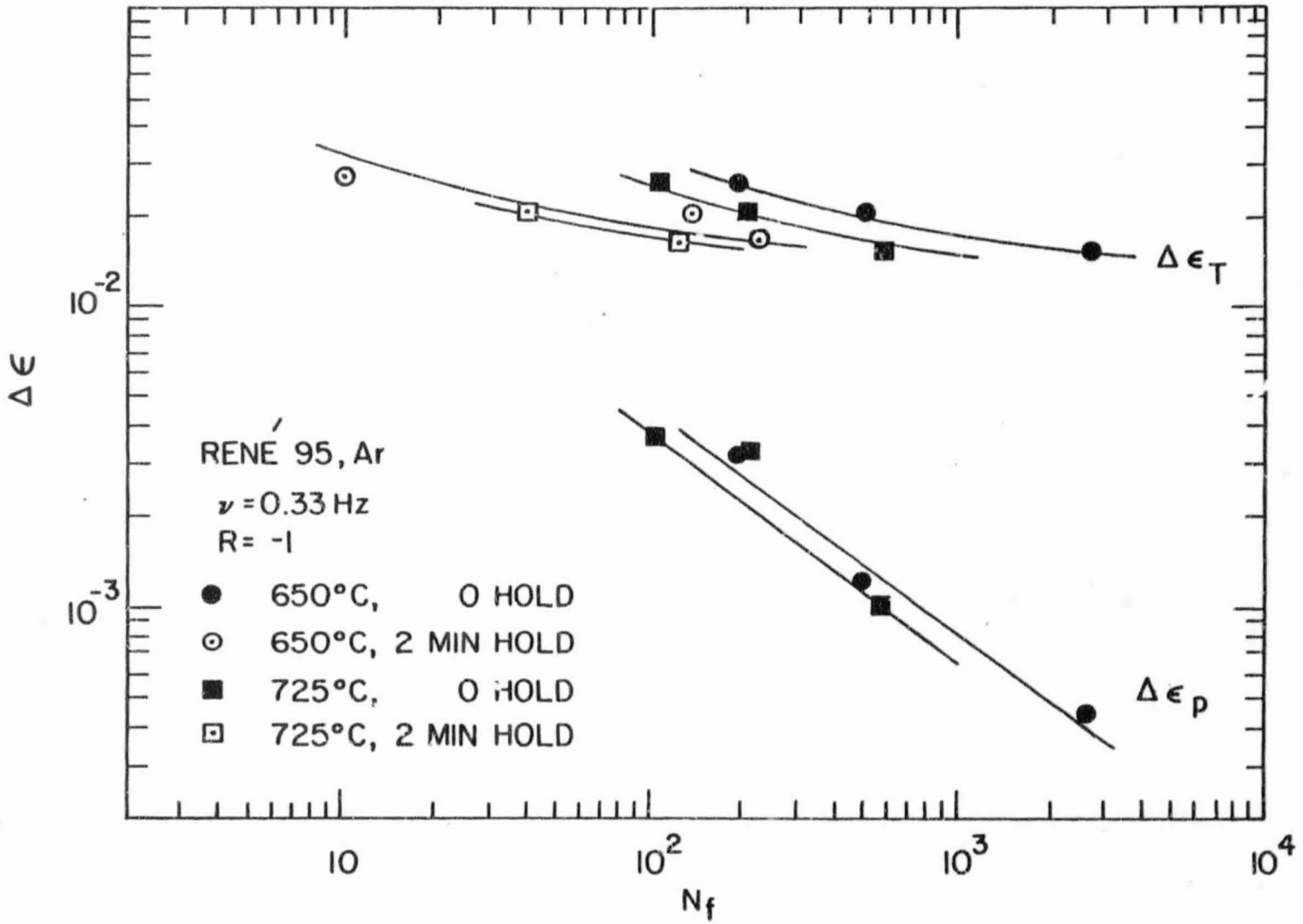

Fig. 20 LCF test results for HIP René 95

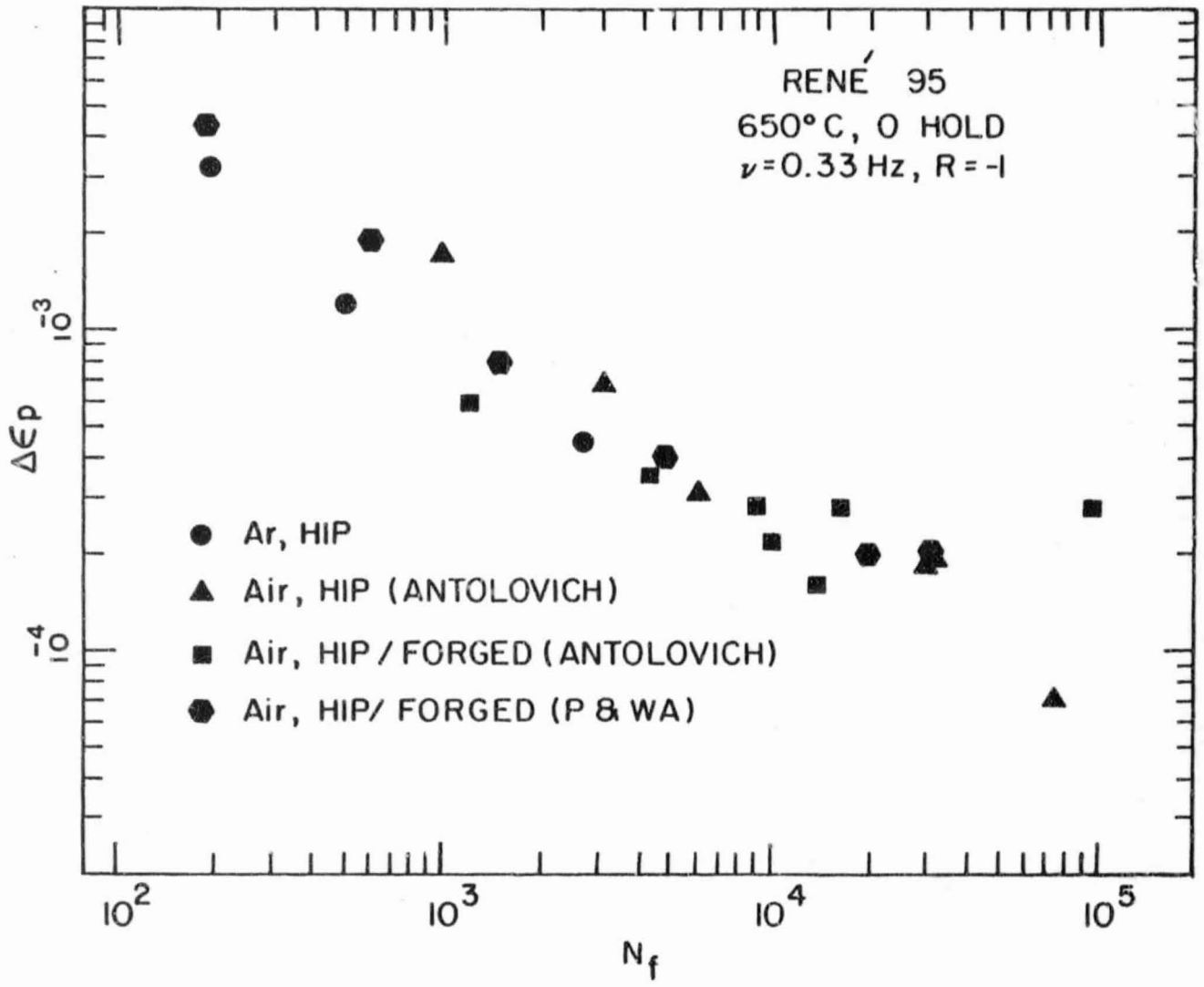

Fig. 21 Coffin-Manson plots for HIP René 95 for comparison with previous results from Refs. 2 and 3

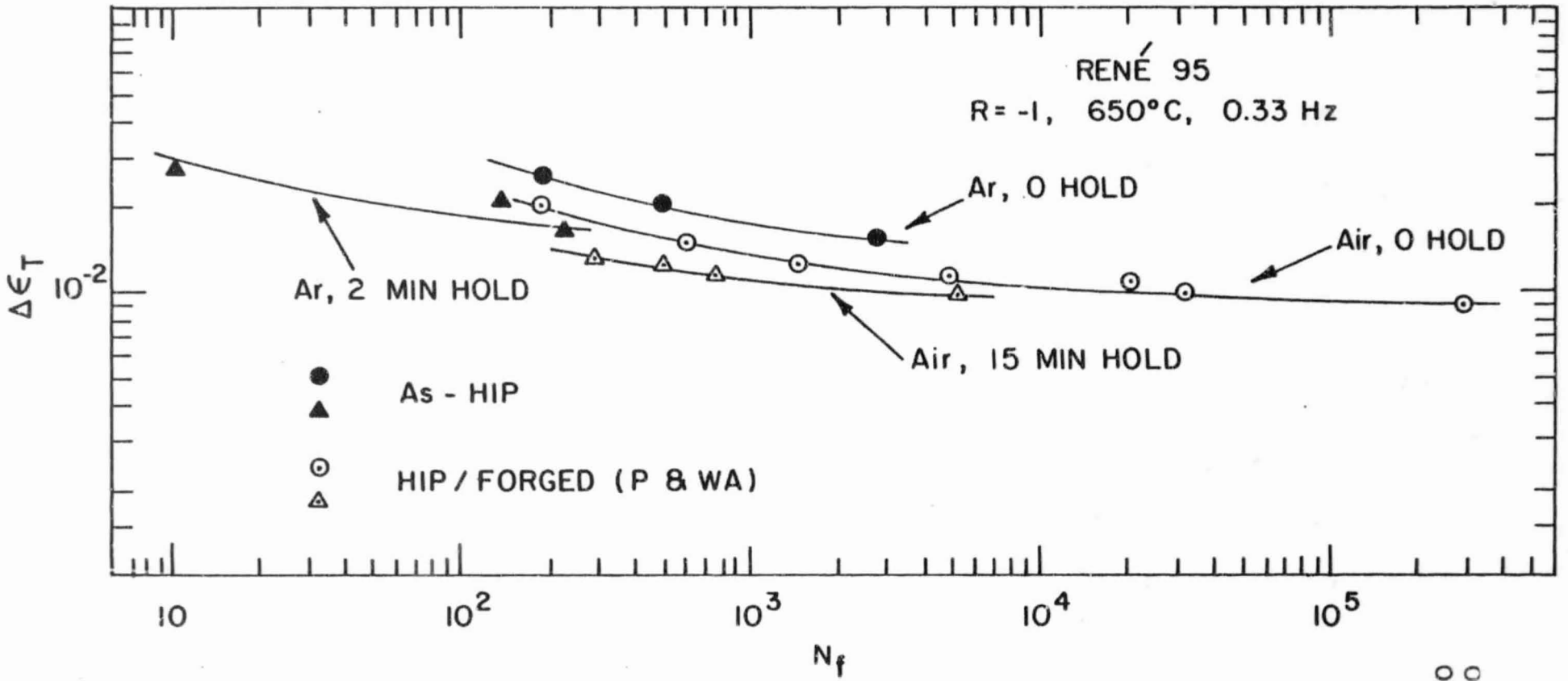

Fig. 22 Strain control LCF results for HIP René 95 for comparison with HIP/FORGED René 95 test results, Ref. 3

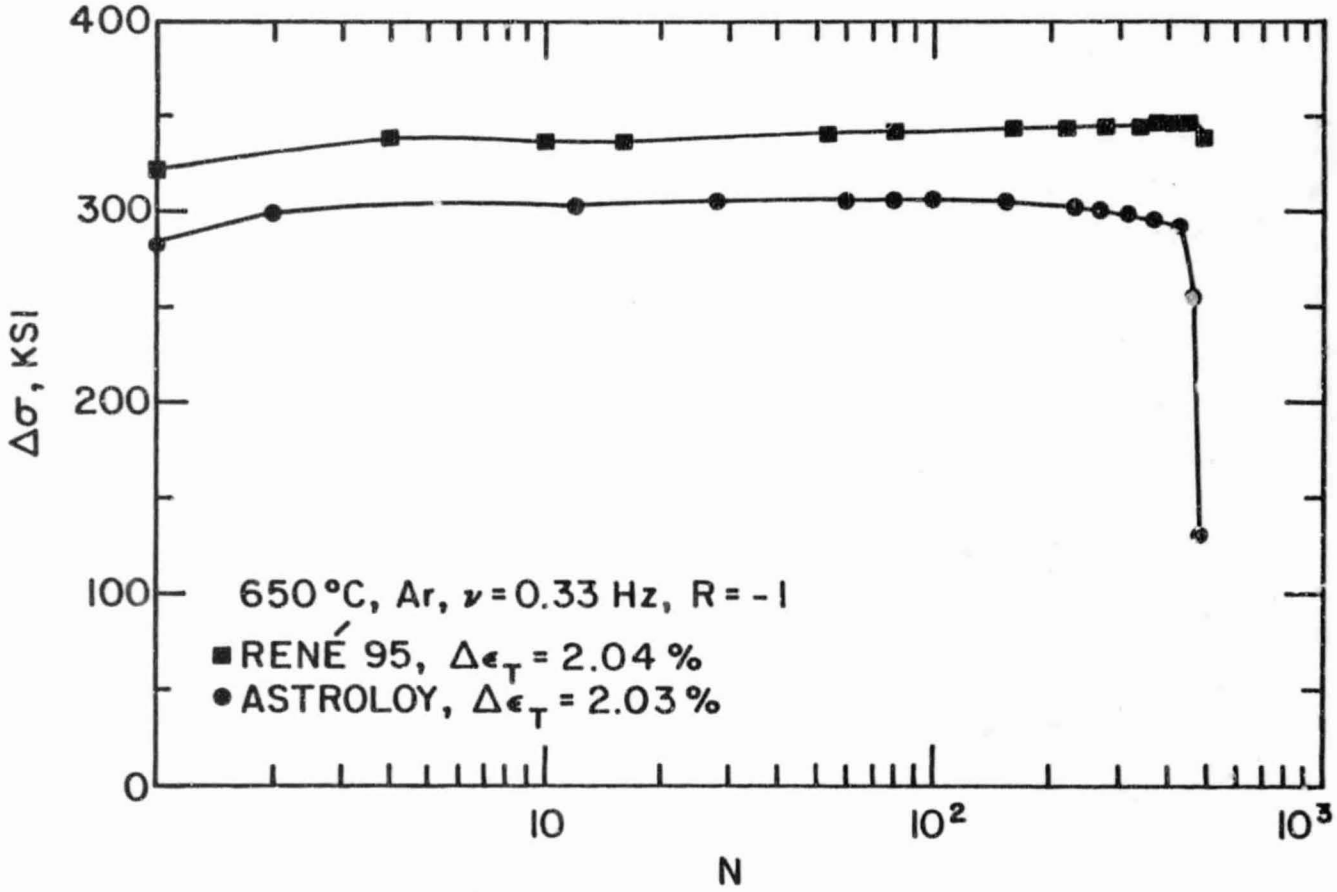

Fig. 23 Cyclic hardening in Astroloy and René 95 at 650°C

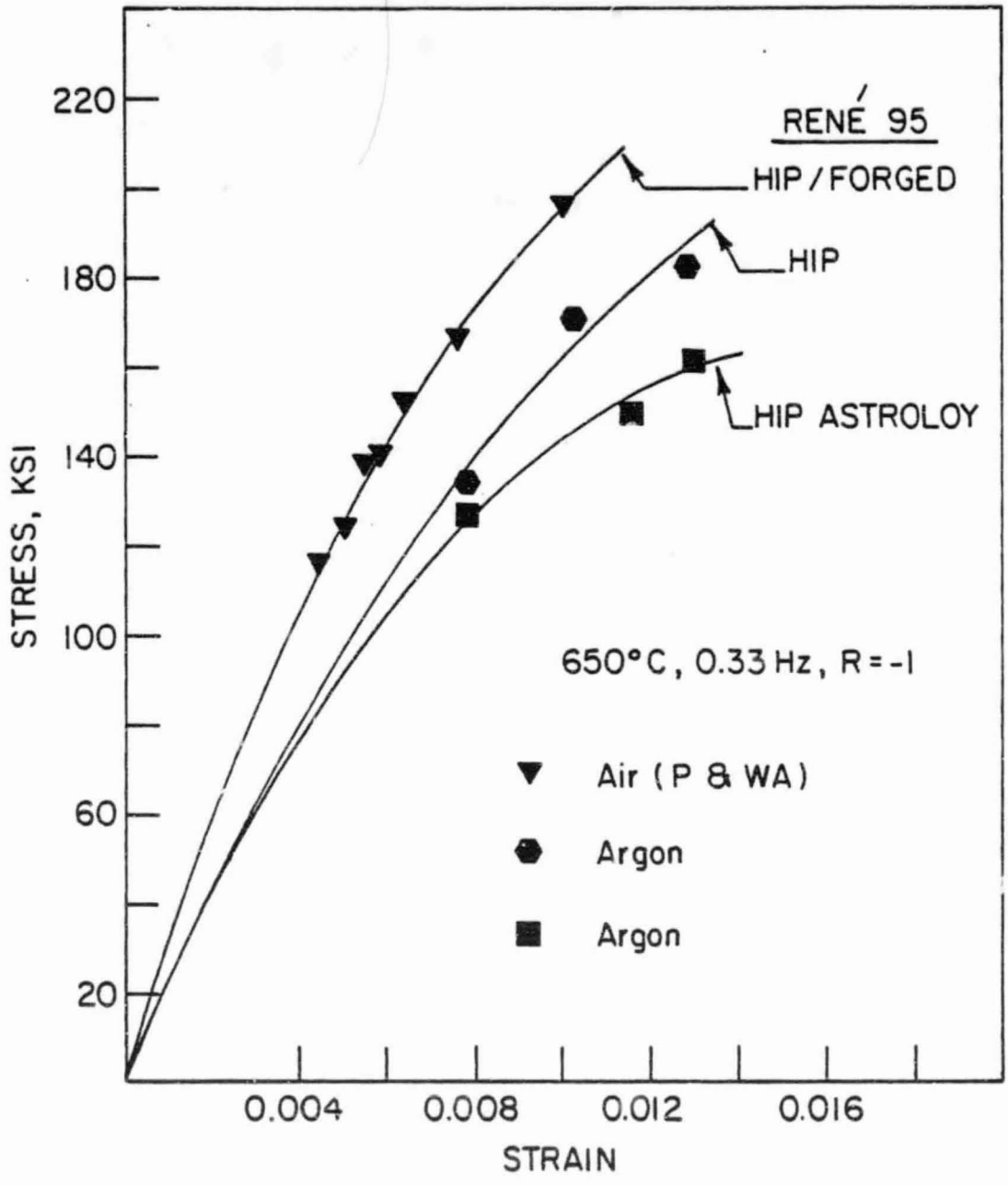

Fig. 24 Cyclic stress-strain behaviors for HIP René 95 and HIP Astroloy for comparison with HIP/FORGED René 95. Data for air from Ref. 3

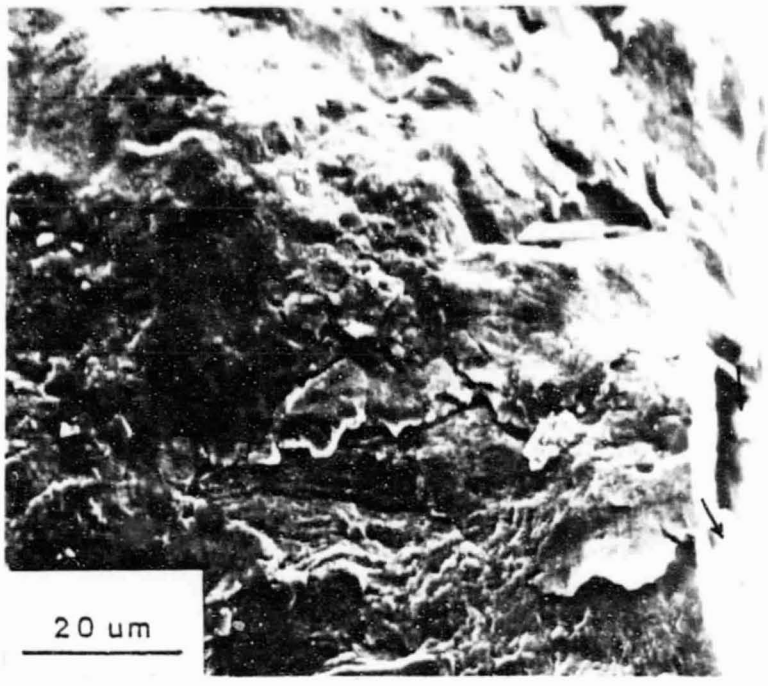

a) Origin (right-hand side is the specimen surface)

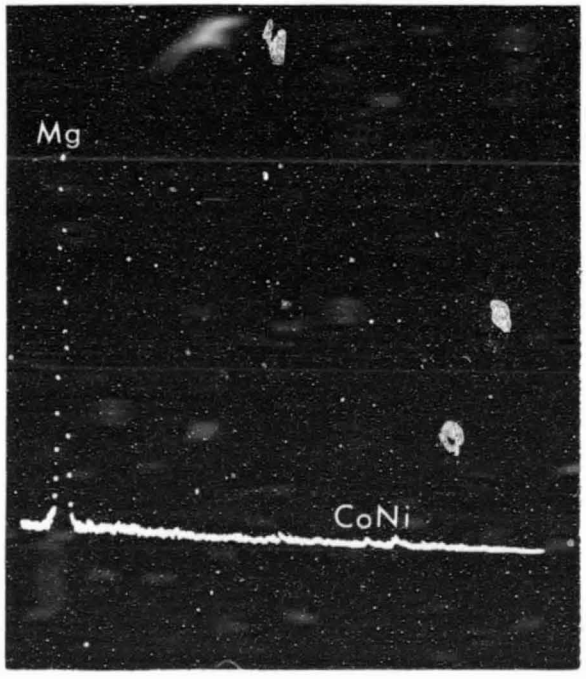

b) X-ray EDS pattern for particles (arrows)

Fig. 25 SEM fractographs of HIP Astroloy, 650°C, $\Delta\varepsilon_t$= 1.56%, 0.33Hz and 0 hold

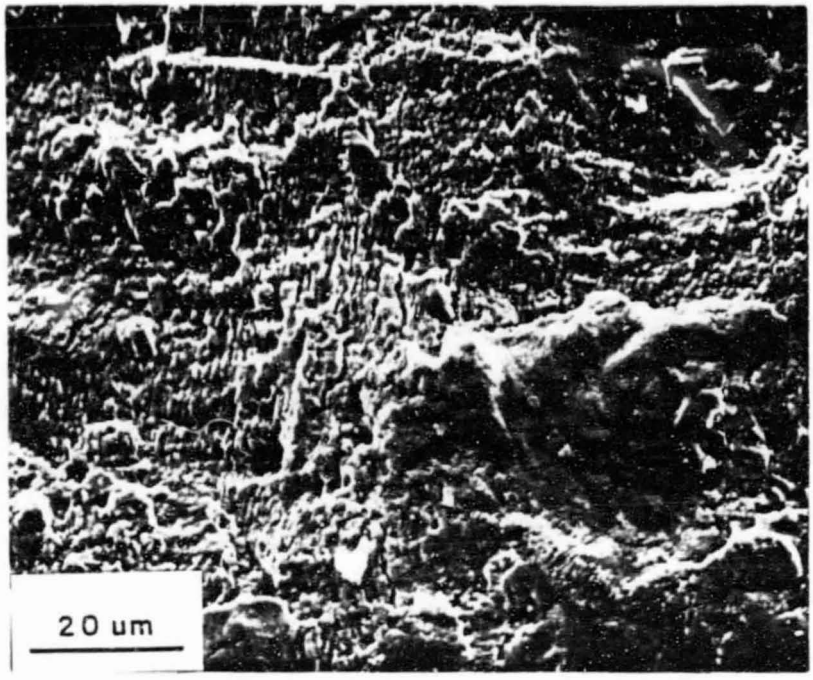

Fig. 26 SEM fractograph of HIP Astroloy near origin, showing brittle striations, 650°C, $\Delta\varepsilon_t$=1.56%, 0.33Hz and 0 hold

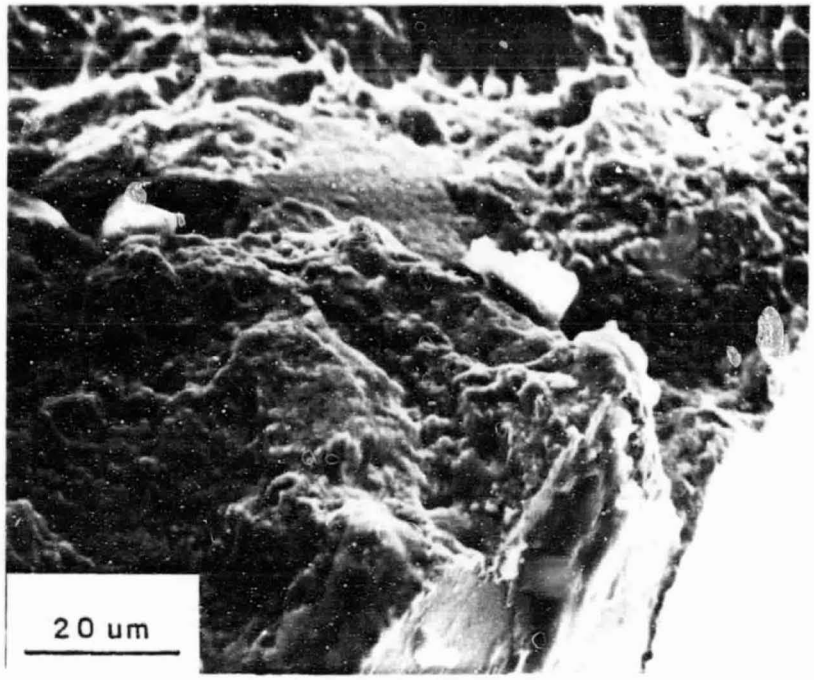

a) origin

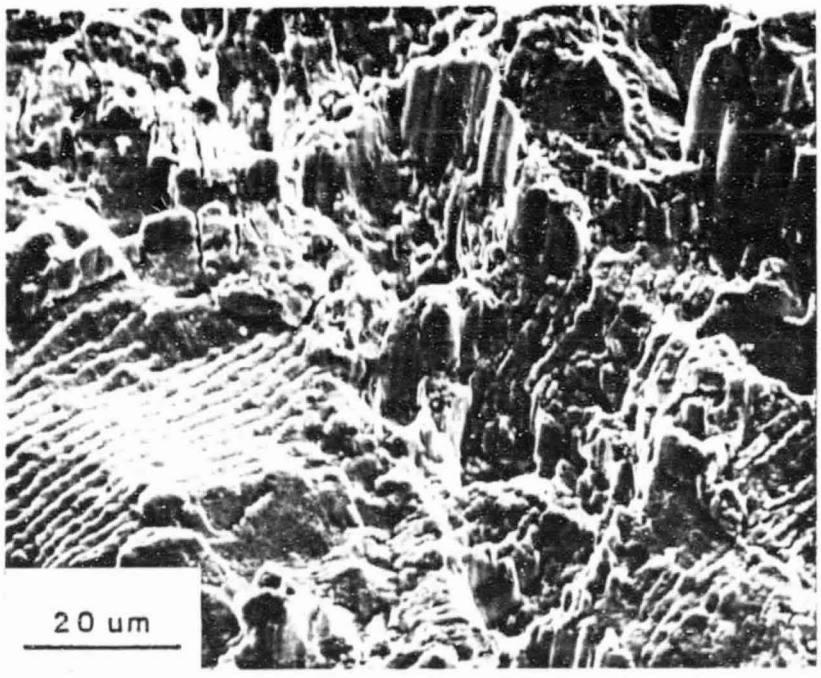

b) crack propagation region near origin showing more readily visible striations and TG+IG cracking

Fig. 27 SEM fractographs of HIP Astroloy, 650°C, $\Delta\varepsilon_t$= 1.67% and 2 min. hold

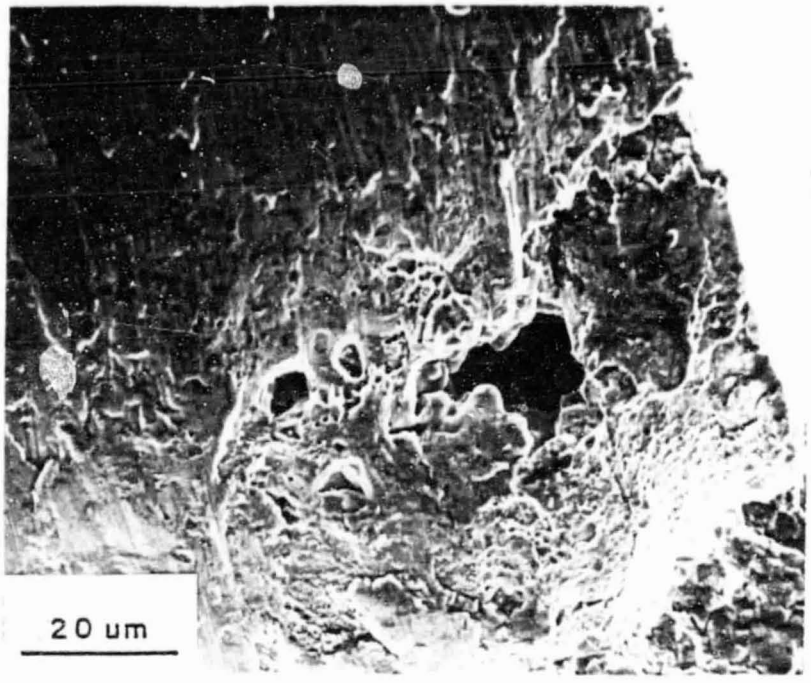

a) Origin associated with pore

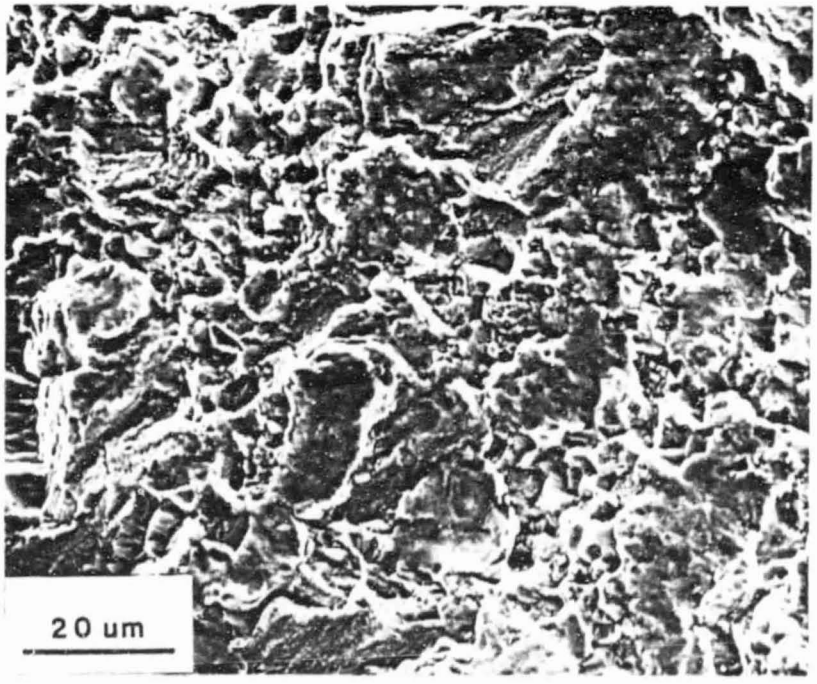

b) Crack propagation region near origin

Fig. 28 SEM fractograph of HIP René 95, 725°C, $\Delta\varepsilon_t$= 1.52%, 0.33Hz and 0 hold

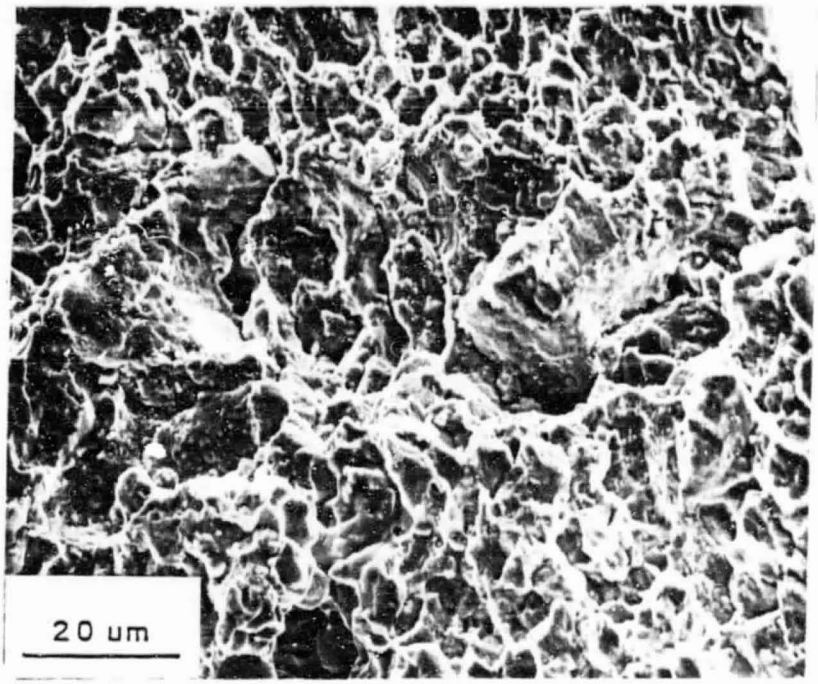

a) origin (right-hand side is the specimen surface)

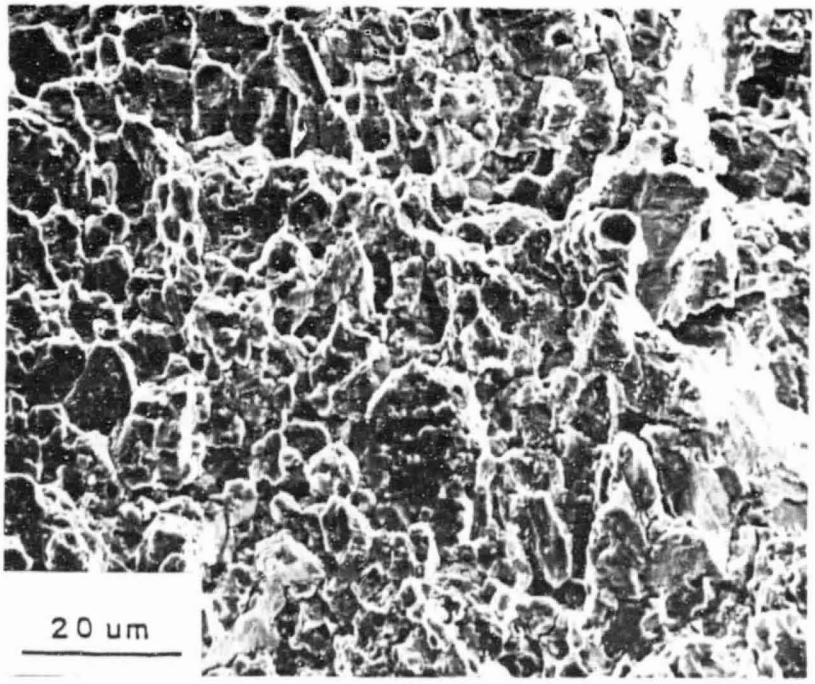

b) crack propagation region near origin

Fig. 29 SEM fractograph of HIP René 95, 650°C, $\Delta\varepsilon_t$= 2.7% and 2 min. hold